ATTACHMENT 2

CONSUMERS POWER COMPANY
PALISADES PLANT
DOCKET 50-255

FLUENCE CALCULATIONS FOR THE PALISADES PLANT

AEAT-0121

April 1996

59 Pages

FLUENCE CALCULATIONS FOR THE PALISADES PLANT

Prepared for

CONSUMERS POWER COMPANY
Jackson, Michigan

April 1996

Prepared By	Date	Quality Assurance	Date
Project Secretary	Date		

AEA Technology
Engineering Services, Inc.
241 CURRY HOLLOW ROAD
PITTSBURGH, PENNSYLVANIA 15236-4696
(412) 655-1200
FAX: (412) 655-2928

2535-4-001-00

AEAT-0121

Fluence Calculations for the Palisades Plant

A F Avery and W V Wright

February 1996

	NAME	SIGNATURE	POSITION	DATE
Author	Wendy Wright	W.V. Wright	Analyst RPSCD	12/3/96
Checker	Alan Avery	A.F. Avery	Shielding Consultant RPSCD	12/3/96
Approver	Colin Cooper	C.A. Cooper	Department Manager, RPSCD	16.3.96

REACTOR PHYSICS, SHIELDING AND CRITICALITY DEPARTMENT
PLANT SUPPORT SERVICES GROUP
AEA TECHNOLOGY
WINFRITH

This report was prepared as an account of work carried out by AEA Technology in accordance with the contract between AEA O'Donnell Inc. and Consumers Power Company dated 10 October 1994.

Fluence Calculations for the Palisades Plant

A F Avery and W V Wright

SUMMARY

Calculations of the neutron fluxes in the pressure vessel of the reactor at the Palisades Plant have been carried out on behalf of Consumers Power Company under the contract between that company and AEA O'Donnell Inc. The calculations have been performed using the MCBEND Monte Carlo code with nuclear data from the ENDF/B-VI library. Values of the neutron fluxes have been obtained in the surveillance capsules within the vessel and in the cavity outside the vessel as well as at positions through the vessel itself. Calculations have been carried out with the source distributions within the core for cycles 1-4, cycle 5, cycles 6 & 7, cycle 8, cycle 9, cycle 10, and cycle 11, the model being changed to describe the modified fuel assemblies in the last four of these cycles. Measurements of the reaction rates of a range of detectors are available from monitors which were removed from surveillance capsules after cycles 5, 9, and 10, and from the cavity after cycles 8 and 9. The calculated and measured reaction rates have been compared and adjustments made to the calculated neutron fluxes in order to improve the consistency between the two sets of values. The fluences are presented in terms of the contributions from neutrons with energies above 0.1MeV and 1.0MeV as well as the displacement rate for iron atoms (dpa).

AEA Technology
Plant Support Services Group
Reactor Physics, Shielding & Criticality Department
Winfrith
Dorchester
Dorset
DT2 8DH

CONTENTS

TABLES

FIGURES

1 INTRODUCTION

Calculations have been performed on behalf of Consumers Power Company to provide values of the neutron fluences in the surveillance capsules and the pressure vessel of the Palisades plant in order to assess the property changes that will be induced by neutron irradiation. The reactor has recently completed its 11th cycle of operation, and the fluences have been obtained based on actual power histories, core loadings, and source distributions for these cycles. Fluences have been derived at the inner and outer surfaces of the vessel and at quarter, half and three-quarter distances through the vessel at the core centre-plane and at 450mm below the centre-plane. Steel specimens have been irradiated in surveillance capsules located inboard of the vessel and fluences are provided at these positions in order to relate the measured property changes in the samples to those that are expected in the vessel itself. Measurements of the reaction rates of a number of detectors have been made in these surveillance capsules and also in dosimetry capsules located in the cavity between the vessel and the primary shield. The calculations include predictions of these reaction rates thus enabling their accuracies to be assessed through comparisons with the measurements.

The geometrical model which was developed for this work was based on drawings of the Palisades plant provided by Consumers Power Company. The calculations were carried out using the radiation shielding code MCBEND9A (1) and nuclear data from ENDF/B-VI processed into the DICE format in 8270 energy bands (2) for use with this code. The code and the data have been validated for use in this type of calculation by comparisons of measured and predicted reaction rates in the H B Robinson PWR and in the NESDIP 2 simulation of a PWR shield (3).

The calculations were performed under the contract between Consumers Power Company and AEA O'Donnell Inc dated October 10 1994.

2 MODEL DESCRIPTION

A three-dimensional model of the reactor, based on the engineering drawings provided, was created for use in the MCBEND code. The geometry was set up using the FG (fractal geometry) facility in MCBEND (1). Advantage was taken of the symmetry of the reactor so that a 90° sector was modelled with reflection planes at the azimuthal boundaries. Since calculations were only required at radial positions close to the core centre plane it was not necessary to include detailed representations of the components at the top and bottom of the core.

A vertical section through the model of the Palisades reactor is shown in figure 1 whilst a plan view across the core is shown in figure 2. Azimuthally a quarter section of the reactor was modelled extending radially to include the first 50cm of the concrete shield, the latter having an inner radius 335.92cm with a 0.64cm thick mild steel liner inside this. In the axial direction it extended from the centre line of the nozzle above the core to 50cm into the base concrete. The reactor core is composed of 204 fuel elements of 366.95cm overall height and 335.28cm active length. The core is surrounded laterally by the core shroud of 1.59cm thick steel and the core barrel. The shroud is stepped to form a wrapper around the fuel assemblies while the barrel is a steel cylinder of height 570.41cm with outer diameter 387.98cm and thickness 3.81cm. Between the core barrel and the shroud there are eight horizontal support plates of 3.81cm thick steel spaced at intervals of 44.45cm, the base of the lowest plate being at 163.59cm below the centre plane of the active core. The carbon steel pressure vessel is formed of a cylinder of wall thickness 21.59cm and outer diameter 481.34cm, the inner surface being lined with 0.64cm stainless steel. The vessel has a dome-shaped base with its centre at 231.80cm below the core centre line. Outside the pressure vessel there is a similarly shaped insulation layer of thickness 10.16cm with outer diameter 505.46cm over the barrel section and outer radius 257.97cm over the domed base. These features

were represented explicitly in the model as shown in figures 1 and 2. (Later data which became available after completion of the calculations showed that a more accurate value for the as-built thickness of the vessel barrel would be 0.76cm (0.3inches) greater than the 21.59cm (8.5inches) specified in the model. The effect of this difference is considered in Section 7.4 below)

The arrangement of the fuel elements within one quarter of the core is shown in figure 3, the elements being numbered according to the reactor scheme. They are square in cross-section (20.955cm x 20.955cm) in a symmetric arrangement with alternating gaps of 0.2667cm and 0.9322cm separating most elements. The gap along the symmetry planes is 0.9322cm. The exceptions to this regular pattern are the elements in the outer rows of three (numbers 8, 16, 24 and 49, 50, 51) which are separated from each other by 0.2667cm gaps. In modelling the core the gaps between assemblies were reproduced explicitly.

The plan views across a fuel pin and a fuel element with 216 fuel pins are shown in figure 4. The fuel element is composed of a 15 x 15 array of pin positions with the central position being filled by a guide tube, and 8 others being occupied by guide rods, there being two in the outer row of pins on each side of the assembly. Other fuel assemblies contain only 208 fuel pins with a further 8 pin positions being occupied by guide tubes. This arrangement is shown in figure 5a. The pin pitch is 1.397cm and each pin is composed of uranium oxide pellets of diameter 0.89cm with zircaloy-4 cladding of outer diameter 1.06cm and thickness 0.075cm. The height of the active length of the fuel is 335.28cm with inactive regions in the assemblies of height 21.06cm at the top and 10.61cm at the base.

The numbers of 216 pin and 208 pin assemblies forming the reactor core varies from cycle to cycle. In addition for cycles 8 to 11 some of the pin positions were occupied by hafnium or steel rods in selected peripheral assemblies. Plan views across the arrangements of the special assemblies are shown in figures 5b to 5e whilst the core loading for each cycle is shown in Table 1. For cycle 8 fuel assemblies with four rows of steel rods as shown in figure 5c were loaded into locations numbered 8, 38, 48, and 49 in figure 3, with corresponding loadings in the other quadrants. In cycle 9 these four positions were occupied by fuel assemblies with hafnium rods as shown in figure 5b. For cycle 10 assemblies with hafnium rods were loaded into positions 24, 38, 48, and 51 while assemblies with the pattern of steel rods shown in figure 5d were installed in locations 8 and 49. For cycle 11 the assemblies with steel rods at their corners as shown in figure 5e replaced those with hafnium rods in cycle 10, and the assemblies with steel rods along two sides were retained at locations 8 and 49. For the inner core the materials within the active length of each assembly were smeared over the corresponding volume. For those assemblies at the edge of the core the modelling was more detailed with the materials being smeared over each pin cell to give appropriate compositions for cells containing fuel, guide tubes, guide rods, or steel rods.

The surveillance capsules have been modelled as rectangular steel rods 3.89cm x 1.95cm in cross-section and 366.95cm in height located centrally in a 4.92cm x 3.21cm x 366.95cm water filled enclosure of 0.305cm thick steel, as shown in figure 6. The capsule was situated at the 20° position just inside the pressure vessel wall, with its centre at a distance of 214.63cm from the core axis, and it was present in the calculations for all cycles. An accelerated capsule, modelled as for the surveillance capsule, was present in the model for the calculations for cycles 1 to 5, being located on the outer surface of the core barrel at the 30° position with its centre at 196.19cm from the core axis. (The azimuthal angles defining these positions are measured in a clockwise direction relative to the 0° axis shown in figure 2.)

Scoring regions were set up in which the Monte Carlo calculation gave mean values of the fluxes and reaction rates. For the surveillance capsules these were axial regions of 50cm length in the steel representing the samples. In the vessel wall scoring regions of

50cm height, 5° angle and 1cm thickness were set up at positions at quarter, half and three-quarters penetration and at the outer surface. At the inner surface scoring was in similar azimuthal and axial intervals over the thickness of the vessel liner. Fluxes and reaction rates were also scored in the cavity at the positions of the dosimetry capsules. For cycle 8 the scoring regions were at the nominal radial position of 108inches (i.e. having boundaries at 273.82cm and 274.82cm) with heights of 50cm and azimuthal angles of 5°. More detailed scoring regions were included in the model for cycle 9 to take account of the variation in the radial positions of the detectors at various azimuthal angles. 1cm thick scoring regions were therefore set up with inner radii at 255.28cm, 257.56cm, 259.85cm, 262.39cm, 266.96cm and 273.82cm, the heights again being 50cm and the azimuthal extents being mostly 5°.

3 MATERIAL COMPOSITIONS

The compositions of the materials used in the calculations as derived from data supplied by Consumers Power (4) are listed in Table 2. The density of the core water and that of the water between the core shroud and barrel was $0.754 g.cm^{-3}$, and that of the downcomer water was $0.767 g.cm^{-3}$. The densities of the fuel element smears were derived from the table of the masses of materials in the active lengths of the assemblies (4) (5). For the inner fuel assemblies the material was smeared over the whole assembly. For the twelve outer fuel assemblies in the 90° sector, i.e. those with surfaces adjacent to the core shroud, the materials of the fuel pin were smeared with the water over one pin pitch with the guide tubes, guide rods, steel rods and hafnium rods being treated in a similar way.

4 SOURCES

Average pin powers for each cycle, pin powers at 5 time steps through each cycle and combined mean pin powers over cycles 1 to 4 and 6 to 7 were supplied by Consumers Power (5). The pin powers for each fuel assembly were given together with their axial variations in 25 equal lengths over the height of the core. The fractions of the fissions occurring in uranium and plutonium were also supplied for each assembly for the same time steps. The calculations were carried out for a full reactor power of 2530MW (5).

The source in each pin is derived from:

$$\text{Source/cm}^3 = \frac{P.r}{A.l} \times \frac{(2.432f_U + 2.88f_{Pu})}{(3.242E-17 \times f_U) + (3.385E-17 \times f_{Pu})}$$

where

P is the pin power in MW,
r is the axial profile factor for the assemb
A is the pin area,
l is the active fuel length,
f_U the fraction of fissions in uranium and
f_{Pu} the fraction of fissions in plutonium.

The weighting factors 2.432 and 2.88 are the numbers of neutrons per fission for thermal neutron fission in U^{235} and Pu^{239} taken from ENDF/B-VI, while 3.242E-17 and 3.385E-17 are the corresponding useful energies per fission (MW) taken from the compilation of James (6).

P, the pin power in MW, is given by:

$$P = \frac{2530}{n}.p$$

where n is the number of pins in the reactor and p is the pin power which was normalised to a mean value of unity over the whole core in the distributions provided by Consumers Power.

For most of the fuel elements the source has been averaged across the area of the fuel element. For the fuel assemblies close to the periphery of the core, namely numbers 8, 16, 23, 24, 31, 36, 37, 38, 43, 46, 47, 48, 49, 50, and 51 in figure 3, the source has been represented in greater detail. For cycles 1 to 7 the sources were averaged over a 3 x 3 fuel pin mesh except for the outer three rows of pins adjacent to the core shroud. For these rows the interval for the source mesh was one pin cell in the direction perpendicular to the outer surface so that the areas were 3 x 1 pin mesh in most assemblies but 1 x 1 pin mesh at the corners of the core in assemblies 24, 38, 48, and 51 which have two external surfaces. Similar approaches were followed for the other cycles but the boundaries in cycles 8 and 10 were adjusted slightly to take account of the absence of sources in the steel pins. The calculations are more sensitive to the power distributions in the outer assemblies and the latter show greater variations across an assembly so that the use of the finer mesh enabled the sources to be represented in detail in the important regions. Separate calculations were performed for the sources in the inner and outer assemblies with single axial profiles being applied in each case. These corresponded to the mean axial profiles for the two sets of assemblies.

The fraction of the source neutrons arising from fissions in plutonium for each assembly was calculated from:

$$\frac{2.88 f_{Pu}}{2.88 f_{Pu} + 2.432 f_U}$$

where f_{Pu} is the fraction of fissions for plutonium and f_U is the fraction of fissions for uranium in the assembly.

The total sources for each cycle or combination of cycles used in the calculations are shown in Table 3.

The spectra of neutrons arising from fission in U^{235} and Pu^{239} were generated by the in-built capability of MCBEND, and sampled using the appropriate fractions for the contributions of the two isotopes to obtain the variation of the total source with energy.

5 CALCULATIONAL METHOD

The calculations were carried out using version 9A of the Monte Carlo code MCBEND (1) with data taken from the ENDF/B-VI neutron cross-section library (2). The reaction rates were calculated using the IRDF-90 cross-sections (7) for the detectors and the data from ASTM Standard E693-79 for the dpa rate, these being held in all cases in the 640 energy groups of the SAND II scheme. The code and data are maintained to a level of quality assurance consistent with the standards of the ANSWERS Software Service of AEA Technology. This ensures that reference versions of the code, data libraries and test data are held, and that updating and archiving of the code and data are strictly controlled. The neutron fluxes were calculated in a standard 30 group energy scheme as shown in Table 4.

The quantities of interest are the neutron fluences above 0.1MeV and 1.0MeV, and the displacement rates per atom in iron (dpa) in the vessel at the core centre plane and in the circumferential weld at about 45cm below the core centre. They were calculated at the inner and outer surfaces of the vessel, and at penetrations of one quarter, one half, and three-quarters of the wall thickness through it. Dosimetry reaction rates for all cycles were calculated for the surveillance and accelerated capsules for the reactions $Cu^{63}(n,\alpha)Co^{60}$, $Fe^{54}(n,p)Mn^{54}$, $Ni^{58}(n,p)Co^{58}$, $U^{238}(n,f)X$ and $Ti^{46}(n,p)Sc^{46}$. For cycle 9 the reaction rates for $Co^{59}(n,\gamma)Co^{60}$ and $Np^{237}(n,f)X$ were also obtained in the surveillance capsule although these have not been included in the later analysis. For cycles 8 and 9 dosimetry measurements had been made in the cavity between the vessel and the primary shield with $Cu^{63}(n,\alpha)Co^{60}$, $Fe^{54}(n,p)Mn^{54}$, $Ni^{58}(n,p)Co^{58}$, $U^{238}(n,f)Cs^{137}$, $Ti^{46}(n,p)Sc^{46}$, $Nb^{93}(n,n')Nb^{93m}$, $Co^{59}(n,\gamma)Co^{60}$ and $Np^{237}(n,f)Cs^{137}$, and the reaction rates for these detectors were therefore calculated in the cavity regions. The calculated reaction rates for Co^{59} have not been used in the subsequent comparisons with measurements because of the sensitivity of the values to the rather uncertain composition of the concrete primary shield, and the low relevance of the neutrons to which this detector is sensitive in assessing the accuracies of the fluxes at higher energies which are important for radiation damage. The fluxes and the reaction rates were scored by track length estimation to give the mean values over the volumes described in Section 2 above. The detailed pattern of scoring regions within the cavity for cycle 9 enabled the reaction rates to be calculated at the positions of the detectors. The distributions within the cavity also gave factors which could be applied to allow for the differences between the true positions of the detectors and the nominal position of 108 inches from the core axis for cycle 8.

For convenience in specifying the source distributions the calculations were performed separately for the inner (numbered 1, 2, 3, 4, 5, 6, 7, 9, 10, 11, 12, 13, 14, 15, 17, 18, 19, 20, 21, 22, 25, 26, 27, 28, 29, 30, 32, 33, 34, 35, 39, 40, 41, 42, 44, 45 in figure 3) and outer (8, 16, 23, 24, 31, 36, 37, 38, 43, 46, 47, 48, 49, 50, 51) fuel elements, and the results combined. Calculations were performed for sources from cycles 1 to 4 combined, cycle 5, cycles 6 and 7 combined, and for cycles 8, 9, 10 and 11. Cycle 5 was calculated separately because it preceded the removal of dosimetry from the surveillance capsule and would thus have a major effect on many of the calculated activations of the detectors. When calculating the integrated fluences for several cycles it is possible to use the average source distributions for those cycles, but more detailed consideration is needed for the reaction rates of the short-lived isotopes (e.g. Co^{58} with its half life of 70.8 days) because these will only be sensitive to the fluxes in the year before removal. In an initial study three calculations were performed for cycle 8 for the distribution of pin powers at the beginning, middle and end of the cycle (referred to as times 1, 2 and 3) and activations of the detectors were calculated using the time-dependence of the reaction rates through the cycle. However the differences between this approach and the use of cycle-averaged reaction rates were about 1% so that time dependence of the source distributions within a cycle was not included in any of the other calculations. For cycles 5, 9, 10 and 11 therefore the average pin powers over each of the cycles were used There were significant differences in the arrangement of the pins in the peripheral sub-assemblies for cycles 8, 9, 10, and 11 which necessitated separate treatments for each. For cycle 8 the sensitivity module in MCBEND was used to obtain the rates of change of the calculated fluxes and reaction rates with changes in the cross-sections. These could then be combined with the co-variance data for the cross-sections to derive the uncertainties in the predictions due to uncertainties in the cross-sections.

The acceleration of the MCBEND calculations was achieved with splitting and Russian roulette together with automatic weighting of the source. The importances were calculated in an initial run using the MAGIC option of MCBEND.

6 MEASUREMENTS

Measurements had been made of the reaction rates of a number of detectors that had been irradiated in surveillance capsules located at the 20° position. Dosimetry packs were removed at the end of cycles 5, 9, and 10, the detectors having been irradiated over all preceding cycles for the first and last of these, but only for cycle 9 for the other. Dosimetry packs were also irradiated in the cavity outside the pressure vessel at a number of azimuthal positions in cycles 8 and 9. Details of the detectors are summarised in Table 5. The values of the decay rates of the reaction products were measured and presented as dps/gm of foil material corrected to consistent dates for the four sets. These were 27 June 1984, 12 December 1990, 4 March 1992, and 12 October 1993 respectively for the measurements after Cycles 5, 8, 9, and 10. Values of the decay rates as supplied by Consumers Power are given in Table 6, these being the measurements made at the centres of the capsules for detectors other than the fission foils. The table also includes the reference numbers for the capsule and for the individual monitor foils on which the quoted reaction rates are based. Where several detectors of the same type were counted the value given in Table 6 is the arithmetic mean. For $U^{238}(n,f)$ the values given previously have now been corrected for U^{235} impurities, photofission and the build up of plutonium, whilst for $Np^{237}(n,f)$ the measurements have been corrected for photofission (8). Values of the mean saturation reaction rates for the fission detectors after being corrected are given in reference 8, but the individual correction factors for each detector are not available. The saturated values have been converted into decay rates on the specified dates for inclusion in Table 6 by applying in reverse the formula that was used in the averaging process. Values of the parameters in this formula were taken from reference 8. The original measurements were made by determining the decay rates for three different fission products in each case, but the results presented in reference 8 are mean values of the fission rates. It is not possible therefore to derive the individual activities measured for the three isotopes and the results are shown in Table 6 for $U^{238}(n,f)Cs^{137}$ only as being typical for all of them. (The values of the ratio of "Calculated Activity"/"Measured Activity" (C/M) are independent of the choice of isotope for converting from saturation activity to measured activity.)

The positions at which the dosimetry packs were irradiated in the cavity are summarised in Table 7. The support bar from which they were suspended was misaligned so that the capsules at 6° were closer to the vessel than those at 39° by 117mm. The angular positions are given relative to the 0° axis shown in figure 2.

7 RESULTS

7.1 Surveillance Capsules

The results of the calculation for the fluxes and activities of the detectors in the surveillance capsule are presented in Table 8 together with the measured decay rates and the ratios of calculation/measurement (C/M). The values of the fluxes and the dpa rates are those for the last cycle of the irradiation. The calculated activity at the specified time for the measurement of a given detector has been derived using the power history of the reactor as given in Table 9 together with the data for the foils as summarised in Table 5 and takes account of the contributions arising from each of the cycles for which the detector was irradiated. The values of C/M range from 0.86 to 1.21. However it can be seen that there is a consistent pattern for each capsule. The C/M ratios for the Fe, Ni, and U^{238} monitors are about 25% higher than those for Cu in all cases while those for Ti lie between the values for Cu and those for the other three detectors. The energy ranges to which the reactions are sensitive are shown in Table 10 which gives the percentage contributions to the reaction rates for neutrons in each of the energy groups. It can be seen that Cu shows the greatest response to neutrons at energies above 6MeV whilst the Fe, Ni and U are more sensitive to neutrons below 3.68MeV. The

contributions to the Ti reaction rate are mostly in the range 3.68 to 10 MeV. This suggests that the calculated neutron spectrum is in error with fluxes being too low at energies above 7.8MeV and too high in the range 0.82MeV to 3.68MeV. In addition to the relative values of C/M for the five detectors there is also a variation from capsule to capsule in the absolute values for a given detector which suggests that the accuracy of the specified source strengths varies. There is however no consistent trend in C/Ms with the half-lives of the detectors; the Ni and Fe reaction products with their differing half-lives of 70.8days and 312days show identical C/Ms which indicates that the time dependence of the neutron fluxes is being treated in sufficient detail. In these circumstances the application of an adjustment procedure to improve the agreement between measurements and calculations is justified.

7.2 Adjustment of the Surveillance Capsule Fluxes

The code SENSAK(9) has been applied to the fluxes calculated at the surveillance capsules in order to adjust the values to bring the predicted reaction rates into closer agreement with those that were measured. The code follows the procedure given in ASTM Standard E 944 in which a maximum likelihood approach is applied. The fluxes and the detector cross-sections were specified in the 30 group scheme of Table 4. Uncertainties of 5% were attributed to the measurements as specified for the dosimetry removed after cycle 5. The contributions to the uncertainties in the calculated flux spectra arise from the fission source spectrum, the material cross-sections, the density of the coolant, the dimensions of the reactor, and the Monte Carlo statistics. Following the analysis for the simulated PWR shield in the NESDIP 2 experiment (10) an uncertainty of 3.5% is estimated to arise from the fission spectrum. Sensitivity calculations were carried out for the dependence of the reaction rates upon the cross-sections of the materials and folded with the co-variance data from the data library. (For hydrogen and oxygen there are no co-variances in ENDF/B-VI so that data from ENDF/B-V were used for these elements.) The resulting uncertainty on the reaction rates was 2.4%. An uncertainty of 2% is estimated for the density of the coolant and the sensitivity calculations showed that this was equivalent to a 5% uncertainty in the reaction rates. The uncertainty in the inner radius of the pressure vessel is 0.25inch (11) which translates into 4.5% in the reaction rates when this is converted into an equivalent change in the thickness of the water between the core and the vessel and the calculated sensitivities are applied. The combination of these effects leads to an uncertainty of ±8% to be added to the statistical uncertainties on the group fluxes. The latter range from 4% in the groups between 1.74MeV and 6.07MeV to 20% in the group between 10.0MeV and 12.0MeV. The standard deviations on the detector cross-sections were taken from the IRDF90 files. An uncertainty of 5% was applied to the source strength, this being the estimated accuracy of the powers specified in the peripheral fuel assemblies. Correlation factors of 0.5 and 0.25 were applied to the group fluxes for the adjacent and next-adjacent groups following the recommendation of McCracken (9). The fluxes in 30 energy groups from the results for cycles 5, 9, and 10 were fed as input to the three SENSAK runs together with the corresponding values of C/M for the detector decay rates from Table 8. Application of the SENSAK code led to increases in the fluxes in the high energy groups coupled with reductions in those at lower energies. Source normalisation factors of 0.98, 0.96, and 0.99 respectively were derived for the calculations for cycles 5, 9, and 10. The adjusted results are summarised in Table 11. It can be seen that the values of C/M after adjustment are mostly within ±5% of unity, this being the standard deviation assigned to the measurements. The exceptions are the reaction rates for Cu after cycle 5 and Ti after cycle 9. The uncertainties are those assigned to the adjusted values by the SENSAK code taking account of the degree of agreement between the measurements and the modified calculations. Table 12 gives the reaction rates and the fluxes in the surveillance capsules for each of the seven time periods for which calculations were performed. The reaction rates are those which were used when deriving the activations of the detectors as presented in Table 8. (The activations are the decay rates of the detectors at a specific date after removal from the reactor and they take account of the

contributions from activation during each cycle for which the detectors were irradiated and of the subsequent decay. The reaction rates in Table 12 give the rates of production of the active isotopes which are used when calculating these contributions. They correspond to the activations that would be produced if the reactions were saturated with zero decay.) In addition Table 12 includes the fluences for each period derived from the fluxes using the equivalent full power seconds (EFPS) from Table 9 for each cycle. These fluences are also presented as the cumulative values through the operation of the plant to date. Finally Table 12 includes adjusted values of the cumulative fluences obtained using mean values of the adjustment factors for each of the responses ϕ>0.1MeV, ϕ>1.0MeV and dpa (see Section 8 below). Table 13 gives the axial variation of the fluences integrated over cycles 1 to 11.

7.3 Fluxes in the Cavity

The results for the calculations of the fluxes and reaction rates in the cavity for cycles 8 and 9 are summarised in Table 14. The results for cycle 9 were calculated at the positions of the dosimetry packs; those for cycle 8 were obtained at the nominal radius of 108inches and converted to correspond to the positions of the measurements by multiplying by the ratios from the calculated pattern of reaction rates in the cavity for cycle 9. The factors for correcting for the change in position ranged from 0.97 to 1.15 which is indicative of the variation in a reaction rate with radial position within the cavity, and also of the uncertainty arising when the position of the detectors is not known accurately. The ratios of calculations to measurements are summarised in Table 15. There is again a trend in the C/Ms with the values for Fe, Ni and U^{238} tending to be higher than those for Cu, although it is not so marked as was the case for the surveillance capsules, and is completely absent for the results at 39° for cycle 8. In the latter comparison the values of C/M lie between 0.96 and 1.06 with no consistent variation with the energy range to which the detectors are sensitive. For the remainder the mean ratio between the C/Ms for Cu and those for Fe and Ni is 0.9 compared with the corresponding value of 0.8 for the surveillance capsules. The shape of the neutron spectrum is thus predicted more accurately for the cavity dosimetry than it was for the capsules. However the overall mean value of C/M is 1.14 when all of the results in Table 15 are included, which can be compared with the corresponding mean of 1.06 for the surveillance capsules.

The energy distributions of the contributions to the reaction rates in the cavity are presented in Table 16 for three azimuthal positions for cycle 8. The neutron spectrum is softer than it is in the surveillance capsules with 30% of the U^{238} reaction rate arising from neutrons with energies below 1.74MeV compared with 14% for the positions inside the vessel. Correspondingly the fraction of the flux at energies above 1MeV which is below 1.74MeV is 63% in the cavity compared with 30% in the surveillance capsules. The U^{238} reaction rate is thus more important as an indicator of the accuracy of the calculated ϕ>1.0MeV in the cavity than it was in the capsules.

7.4 Adjustment of the Fluxes in the Cavity

The SENSAK code has been used to adjust the neutron fluxes in the cavity following a similar procedure to that adopted when modifying the results for the surveillance capsules. The uncertainty to be added to the statistical uncertainties for the group fluxes was increased to 21%. This was due to the additional contribution of the uncertainty in the calculated attenuation by the pressure vessel arising from the co-variance data for the cross-sections of iron, a tolerance of 0.25inches on the thickness of the vessel (11), and the sensitivities of the reaction rates to the iron cross-sections. The statistical uncertainties on the group fluxes were between 1.8% and 6.3% for the energy range between 0.01MeV and 10MeV with larger uncertainties for the groups above this. The uncertainties for the measurements with the U^{238} and Np^{237} fission foils in the cavity were relaxed from 5% to 10% in view of the large differences between the C/Ms for the two detectors in the results for cycle 8. The adjusted values of ϕ>0.1MeV, ϕ>1.0MeV,

and the dpa rate together with the modified C/Ms are summarised in Table 17. The adjusted values of C/M are mostly within 1% of unity with a few showing discrepancies of 2% and 3%. The values of ϕ>1.0MeV are reduced by factors in the range 0.78 to 0.97 with the adjustments leading to smaller changes for ϕ>0.1MeV and the dpa rate. The uncertainties on the adjusted quantities are mostly close to those assigned to the measurements although where there is consistency across the detectors as in the results at 39° for cycle 8 they are reduced. Conversely they are increased above the standard deviations specified for the measurements where the SENSAK code recognises inconsistencies.

After completion of the calculations it was found that a more accurate value for the as-built thickness of the vessel would be 8.8inches instead of the 8.5inch thickness that was used in the model (12). The difference is just greater than the 0.25inch standard deviation assumed in the SENSAK adjustments. However increasing the uncertainty to cover this would give an overall standard deviation of 24% for the calculated reaction rates instead of the value of 21% used above. As most of the adjustments in the cavity are less than 21% it is not expected that an increase of 3% in the uncertainty would change the results significantly. It is estimated that an increase of 0.3inches in the vessel thickness would reduce the reaction rates for energies above 1MeV by 18% which would give a mean C/M for the cavity of 0.96 instead of 1.14. However the decreases in the reaction rates which have been generated by SENSAK will be correcting for this error in the thickness as indicated by the mean reduction of the C/M by 15% for the high energy reactions (i.e. omitting the Np^{237}(n,f) detector since it also responds to lower energy neutrons). Because they have been adjusted to be consistent with measurements the results from SENSAK will thus correspond to the true vessel thickness.

8 BEST ESTIMATE FLUENCES

The fluxes and reaction rates following adjustment by SENSAK as given in Tables 11 and 17 represent the best estimates of those quantities for the quoted positions and cycles. The measurements on which they are based however, are available for a restricted number of positions and irradiation periods. Thus there are only measurements in the cavity for cycles 8 and 9 while the surveillance capsule results refer only to the 20° azimuthal angle. The adjustments to the fluxes are made to allow for errors in the calculations so that the latter are modified to be consistent with the measurements. The nature of these errors determines the way in which they will affect the results at different times and positions.

Errors in the source data may be expected to vary from cycle to cycle especially when the configurations of the important fuel assemblies in the peripheral locations differ. In absolute terms such errors will tend to affect positions at all penetrations through the vessel equally, but variations in the accuracy of the distributions within the outer assemblies will give an azimuthal dependence of the errors arising from the source data.

Errors in the material cross-sections and the fission spectrum will give errors in the calculated fluxes which will be independent of time. They will however be functions of the thicknesses of the materials which have been penetrated; corrections due to shortcomings in the cross-sections for iron for example would be higher at points outside the vessel than at those on the inner surface.

Errors in the dimensions of the vessel will not vary with time but could depend upon position. Therefore adjustments made on the basis of measurements made in one octant of the reactor would not necessarily apply in the other sectors.

Errors in the density of the coolant could change from cycle to cycle but for a given cycle the errors in the fluxes resulting from this source would be expected to be approximately similar at any point within the wall of the vessel or in the cavity.

The statistical uncertainties of the calculations lead to errors which will vary both with position and cycle, although these have been reduced to levels where their contributions are small compared with those arising from the other sources.

The errors can thus be classified as being dependent on time and position either separately or in combination. The measurements for cycles 8 and 9 give evidence of the accuracy of the calculations at specific positions for single core source distributions. The monitors withdrawn with the surveillance capsules after cycles 5 and 10 give data relevant to the fluxes in the capsules for all preceding cycles, but this is restricted to the longer lived detectors. The reactions with the shorter-lived products such as $Ti^{46}(n,p)Sc^{46}$ (half-life 83.8d), $Ni^{58}(n,p)Co^{58}$ (half-life 70.8d), $U^{238}(n,f)Zr^{95}$(half-life 64.2d), and $U^{238}(n,f)Ru^{103}$(half-life 39.4d) will only provide data for the cycle immediately preceding removal. The overall period for cycles 1-5 is nearly 13 years so that it would only be $U^{238}(n.f)Cs^{137}$ (half-life 30.2y) and to a lesser degree $Cu^{63}(n,\alpha)Co^{60}$(half-life 5.26y) which would be sensitive to the early cycles. Similarly for the capsules removed after cycle 10 the total elapsed time of the irradiation is 22 years with cycle 9 finishing 484 days before the end of the irradiation. Moreover the U^{238} measurements have been rejected from this dosimetry so that the data are mostly relevant to cycle 10 only. The adjustment of the fluxes using the full range of detectors as described in section 7 above is therefore dominated by the cycle preceding the removal of the monitors and it was based on the neutron spectra for those last cycles. It is therefore necessary to extrapolate the conclusions in order to derive best estimates for the other cycles.

The adjustment factors from Table 11 for the three sets of dosimetry were as follows:

	ϕ>0.1MeV	ϕ>1.0MeV	dpa
Cycle 5	0.93 (7.2%)	0.91 (7.2%)	0.93 (5.5%)
Cycle 9	0.90 (10%)	0.85 (9.9%)	0.86 (7.5%)
Cycle 10	0.98 (8.8%)	0.96 (9.2%)	0.95 (6.7%)
Mean	0.94	0.91	0.91

The standard deviations quoted above for the cycle data are those calculated by the SENSAK code from the consistency of the results. The mean values are adopted for scaling the results calculated for ϕ>0.1MeV, ϕ>1.0MeV, and the dpa rates at the front of the vessel. These averages are considered to be the best estimates of the corrections for the time-independent errors which arise from the nuclear data and the fission spectrum. The uncertainties assigned to the factors indicate the degree of confidence that can be placed in the adjusted spectra; a value of 10% is conservatively adopted for this uncertainty when applying the mean factors as corrections for the vessel fluxes. The time-dependent uncertainties identified above as arising from the source data, the coolant density, and the Monte Carlo statistics must be added to this. From the distributions of the adjustment factors for the three cycles the standard deviation for the variation with cycle is close to 5% for each of the quantities. This is less than the standard deviation of 7% to 8% obtained when the individual uncertainties estimated in section 7.2 for the time-dependent quantities are combined. Finally there is the uncertainty due to the change in position to different azimuthal locations on the vessel surface. Contributions to this arise from the departure of the pressure vessel radius from its specified value and the azimuthal variation of the neutron source strength in the core. These were estimated in section 7.2 to be 4.5% and 5% respectively. The total

standard deviation on the adjusted fluxes at the front surface of the vessel is thus 13% from the sum of 10%, 5%, 4.5%, and 5%.

The adjustment factors from Table 17 for the fluxes in the cavity are summarised below.

		ϕ>0.1MeV	ϕ>1.0MeV	dpa
Cycle 8	16°	1.0 (7.3%)	0.91(5.0%)	0.97(5.5%)
	26°	0.97(9.1%)	0.85(4.0%)	0.94(6.8%)
	39°	1.0(4.3%)	0.97(5.9%)	0.99(3.8%)
Cycle 9	16°	0.89(6.1%)	0.84(9.5%)	0.87(7.2%)
	26°	0.93(9.2%)	0.87(4.6%)	0.92(6.9%)
	39°	0.96(10.2%)	0.78(10.1%)	0.88(7.5%)
Mean		0.96	0.87	0.93

The mean factors for ϕ>0.1MeV and dpa are close to those for the surveillance capsules with that for ϕ>1.0MeV being 4% lower. This suggests that the calculation of the attenuation of the three quantities by the pressure vessel is performed with no significant deterioration in the accuracy. The factors which were applied to the fluxes at the inner surface are therefore extended to cover all positions within the steel of the vessel. The uncertainties on the adjustment factors for cycle 8 are smaller than the values for the surveillance capsules while those for cycle 9 are closer to the uncertainties at the inner position. The uncertainties on the adjusted fluxes in the vessel due to the contributions considered above for the inner surface are therefore retained at 13% over the full thickness There is however a further contribution which must be added to this uncertainty of 13% due to possible variations in the thickness of the vessel. The uncertainties on the adjusted values of the three quantities should therefore be increased to 18% at the outer surface of the vessel. (The additional uncertainty will not affect the values at T/4, T/2, and 3T/4 since these are measured from the inner surface of the vessel in units of the nominal thickness.)

The best estimate values of ϕ>0.1MeV, ϕ>1.0MeV, and the dpa rates at the core mid-height are given in Tables 18 to 38 for the azimuthal variations at the five positions through the vessel. These are presented for each of the seven time periods for which calculations were performed, i.e. cycles 1-4, cycle 5, cycles 6&7, cycle 8, cycle 9, cycle 10, and cycle 11. They are the results of the MCBEND calculations multiplied by the mean adjustment factors derived above for the surveillance capsules.

The integrated fluences for cycles 1-11 are summarised in Tables 39 to 41. These have been derived with results from Tables 18 to 38 together with the power history of Table 9 for cycles 1 to 10 and a value of 430 EFPD for cycle 11 taken from reference 8.

It is recommended that for assessing the dose to the vessel the adjusted values of the fluences as given in Tables 18 to 41 should be adopted. For the surveillance capsules it is recommended that the adjusted fluences as given in the last three rows of Table 12 should be used when deriving the neutron dose to specimens.

The fluxes at the weld at 450mm below the core centre plane are calculated to be identical to those at the centre plane of the core to within 2% to 3%.

REFERENCES

1 MCBEND User Guide for Version 9A
ANSWERS/MCBEND(94)15

2 Dean C J and Eaton C R. "The 1994 DICE Nuclear Data Library"
AEA-RS 5697

3 Avery A F, Chucas S J, Locke H F and Newbon S. "Calculations of Pressure Vessel Fluence in PWRs Using ENDF/B-VI Data" Proceedings of the 8th International Conference on Radiation Shielding" 1994 pp 667 to 685

4 Letter from Ross D. Snuggerud, Consumers Power, to Steve Chucas, AEA Technology, dated 15 January 1995 together with drawings and a diskette containing pin powers.

5 Letter from Ross D. Snuggerud, Consumers Power, to Steve Chucas, AEA Technology, dated 30 November 1994 together with plant details and the power history.

6 James M F. "Energy Released in Fission" AEEW- M863

7 Kocherov N P and McLaughlin P K
The International Dosimetry File (IRDF-90)
IAEA-NDS-141 Rev 2. October 1993

8 Perock J D and Anderson S L "Reactor Vessel Neutron Fluence Measurement Program for Palisades Nuclear Plant - Cycles 1 through 11"
WACAP-14557

9 McCracken A K "Few-Channel Unfolding in Shielding - The SENSAK Code"
Proceedings of Third ASTM-EURATOM Symposium on Reactor Dosimetry
1979 pp732-742

10 Newbon S "The Analysis of NESDIP 2 with ENDB-B/VI Nuclear Data
AEA RS 5591

11 R D Snuggerud, Consumers Power, message to A F Avery, AEA Technology on 17 January 1996.

12 R D Snuggerud, Consumers Power, message to A F Avery, AEA Technology on 7 March 1996.

Table 1 Types of Fuel Elements per Cycle

Cycle	Number of fuel pins per fuel assembly						
	208 pins	212 pins	216 pins	208 pins + 8 Hf rods	152 pins 4 rows of steel rods one side	160 pins 2 rows of steel rods on 2 sides	202 pins Steel pins at corners
1	20	184					
2	68		136				
3	136		68				
4	144		60				
5	192		12				
6	192		12				
7	152		52				
8	88		100		16		
9	56		132	16			
10	16		180	16		8	
11	16		180			8	16

Table 2 Material Compositions

Number	Material	Density (g/cc)	Composition	Fraction (by weight unless stated)
1	Stainless steel	8.0	Cr Ni Fe Mn	0.19 0.10 0.69 0.02
2	Carbon Steel	7.9	C Mn Si Mo Fe	0.0025 0.0134 0.0028 0.0053 0.976
3	Insulation	0.1545	 Air Stainless steel Al	by volume 0.9794 0.0185 0.0021
4	Water, Core	0.754	 H O	by atoms 0.66667 0.33333
5	Concrete	2.45	H Fe Al Ca Si O Mg C	0.004 0.005 0.003 0.218 0.013 0.529 0.120 0.108
	Uranium		 U235 U238	by atoms 0.01715 0.98285
	Fuel, UO_2	10.2	 U O	by atoms 0.33333 0.66667
	Zircaloy-4	6.55	Zr Sn Fe Cr	0.9824 0.0145 0.0021 0.0010

Table 2 Material Compositions (continued)

Number	Material	Density (g/cc)	Composition	Fraction (by weight unless stated)
6	Fuel element smear (208 pins)	4.286	zircaloy fuel water	0.2058 0.6997 0.09459
7	Fuel element smear (216 pins)	4.406	zircaloy fuel water	0.2035 0.7068 0.08969
8	Pin smear over one pitch		 fuel zircaloy water void	by volume 0.31877 0.11892 0.54782 0.01449
9	Guide rod smear over pitch	3.8612	 zircaloy water	by volume 0.537057 0.462944
10	Air	8.65E-4	N O	0.765 0.235
11	Low density steel	3.6777	Stainless steel	1.0
12	Water, downcomer	0.767	 H O	by atoms 0.66667 0.33333
13	Guide tube smear over pitch	1.4221	 zircaloy water	by volume 0.118920 0.881080
14	Water, shroud/core barrel	0.754	 H O	by atoms 0.66667 0.33333
15	Cycle 9 only Hf rod/guide tube smear	5.91025	 Hf Void Zr Water	by volume 0.197780 0.016937 0.190384 0.594899

Table 3 Total Sources used in the Calculations

Cycle	Inner * Fuel Elements (n/s)	Outer † Fuel Elements (n/s)	Total Source (n/s)
1 to 4	3.645E+19	1.204E+19	4.849E+19
5	3.652E+19	1.333E+19	4.985E+19
6 to 7	3.638E+19	1.325E+19	4.963E+19
8 time 1	4.019E+19	9.214E+18	4.940E+19
8 time 2	3.978E+19	1.012E+19	4.990E+19
8 time 3	3.997E+19	1.054E+19	5.051E+19
9	4.244E+19	7.503E+18	4.994E+19
10	4.235E+19	7.454E+18	4.980E+19
11	4.390E+19	5.939E+18	4.984E+19

* Inner fuel elements are:
1, 2, 3, 4, 5, 6, 7, 9, 10, 11, 12, 13, 14, 15, 17, 18, 19, 20, 21, 22, 25, 26, 27, 28, 29, 30, 32, 33, 34, 35, 39, 40, 41, 42, 44, 45

† Outer fuel elements are:
8, 16, 23, 24, 31, 36, 37, 38, 43, 46, 47, 48, 49, 50, 51

The fuel element numbers are as shown in figure 3

Table 4 30 Energy Group Scheme

Group	Upper Energy (MeV)	Group	Upper Energy (MeV)
1	20.0	16	1.840E-1
2	15.0	17	6.760E-2
3	13.5	18	2.480E-2
4	12.0	19	9.120E-3
5	10.0	20	3.450E-3
6	7.790	21	1.235E-3
7	6.070	22	4.540E-4
8	3.680	23	1.670E-4
9	2.865	24	6.140E-5
10	2.232	25	2.260E-5
11	1.738	26	8.320E-6
12	1.353	27	3.060E-6
13	0.823	28	1.130E-6
14	0.500	29	4.140E-7
15	0.303	30	1.520E-7
	0.184		1.000E-7

Table 5 Data for the Detector Foils

Reaction	Foil Material	Weight Fraction of Target Element in the Material	Abundance of Target Isotope in the Element	Product Half-life	Fission Yield	Cycles after which the Foil was removed from the Plant
$Cu^{63}(n,\alpha)Co^{60}$	Copper	1.0	0.6917	5.26 years		5,8,9,10
$Ti^{46}(n,p)Sc^{46}$	Titanium	1.0	0.0825	83.8 days		5,8,9,10
$Fe^{54}(n,p)Mn^{54}$	Iron	1.0	0.0585	312 days		5,8,9,10
$Ni^{58}(n,p)Co^{58}$	Nickel	1.0	0.6777	70.8 days		5,8,9,10
$U^{238}(n,f)Cs^{137}$	Uranium	1.0	1.0	30.2 years	0.06000	5 in Capsule 8 & 9 in the Cavity
$U^{238}(n,f)Zr^{95}$	Uranium	1.0	1.0	64.2 days	0.05105	5 in Capsule 8 & 9 in the Cavity
$U^{238}(n,f)Ru^{103}$	Uranium	1.0	1.0	39.4 days	0.06229	5 in Capsule 8 & 9 in the Cavity
$U^{238}(n,f)Cs^{137}$	$U^{238}O_2$	0.848	1.0	30.2 years	0.06000	9,10 in Capsule
$U^{238}(n,f)Zr^{95}$	$U^{238}O_2$	0.848	1.0	64.2 days	0.05105	9,10 in Capsule
$U^{238}(n,f)Ru^{103}$	$U^{238}O_2$	0.848	1.0	39.4 days	0.06229	9,10 in Capsule
$Np^{237}(n,f)Cs^{137}$	Neptunium	1.0	1.0	30.2 years	0.06311	8 & 9 in Cavity
$Np^{237}(n,f)Zr^{95}$	Neptunium	1.0	1.0	64.2 days	0.05941	8 & 9 in Cavity
$Np^{237}(n,f)Ru^{103}$	Neptunium	1.0	1.0	39.4 days	0.05380	8 & 9 in Cavity
$Np^{237}(n,f)Cs^{137}$	$Np^{237}O_2$	0.881	1.0	30.2 years	0.06311	9 in Capsule
$Np^{237}(n,f)Zr^{95}$	$Np^{237}O_2$	0.881	1.0	64.2 days	0.05941	9 in Capsule
$Np^{237}(n,f)Ru^{103}$	$Np^{237}O_2$	0.881	1.0	39.4 days	0.05380	9 in Capsule
$Co^{59}(n,\alpha)Co^{60}$	Co/Al alloy	0.0102	1.0	5.26 years		8&9

Table 6 Measured Decay Rates

Cycle	Capsule		Cu(n,a)	Ti(n,p)	Fe(n,p)	Ni(n,p)	U^{238}(n,f)	Np^{237}(n,f)
5	W-290 20° In-vessel	Monitors	84-1762	84-1758	84-1759 84-1763 84-1764A 84-1765 84-1766 84-1767	84-1761		
		D/R dps/a	3.63E-17	9.85E-17	2.80E-15	4.35E-16	2.68E-15	
8	B	Monitors	90-1860	90-1861	90-1858	90-1859		
	Cavity 16°	D/R dps/a	1.13E-19	4.33E-18	2.68E-17	2.87E-17	7.86E-18	1.53E-16
	D	Monitors	90-1886	90-1874	90-1871	90-1872		
	Cavity 26°	D/R dps/a	8.70E-20	3.31E-18	2.00E-17	2.15E-17	5.77E-18	1.14E-16
	G	Monitors	90-1899	90-1900	90-1897	90-1898		
	Cavity 39°	D/R dps/a	6.41E-20	2.35E-18	1.44E-17	1.53E-17	4.40E-18	8.13E-17
9	1A4F	Monitors	92-1146	92-1141	92-1142	92-1145		
	In Vssl 20°	D/R dps/a	5.89E-18	6.60E-16	1.97E-15	3.91E-15	2.75E-16	
	J	Monitors	92-761	92-762	92-759	92-760		
	Cavity 16°	D/R dps/a	7.06E-20	6.85E-18	2.22E-17	4.96E-17	4.42E-18	7.31E-17
	K	Monitors	92-774	92-775	92-772	92-773		
	Cavity 26°	D/R dps/a	6.06E-20	5.79E-18	1.86E-17	4.19E-17	4.32E-18	6.92E-17
	N	Monitors	92-800	92-801	92-798	92-799		
	Cavity 39°	D/R dps/a	4.19E-20	3.94E-18	1.26E-17	2.68E-17	2.56E-18	4.10E-17
8/9	A	Monitors	92-722	92-723	92-720	92-721		
	Cavity 6°	D/R dps/a	1.46E-19	6.37E-18	2.83E-17	4.51E-17	9.90E-18	1.78E-16
10	W-110 20° In-vessel	Monitors	93-4210	93-4205	93-4206 93-4211 93-4212 93-4213 93-4214	93-4209		
		D/R dps/a	3.92E-17	1.88E-16	2.22E-15	1.01E-15		

Decay Rates are those at 27 June 1984 for dosimetry removed after Cycle 5
12 December 1990 for dosimetry removed after Cycle 8
4 March 1992 for dosimetry removed after Cycle 9
12 October 1993 for dosimetry removed after Cycle 10.

The fission rates for the U^{238} and Np^{237} foils are derived from the mean values presented in reference 9 using the Cs^{137} half-life.

Table 7 Positions of the Cavity Dosimetry

Capsule	Angle	Radial Position
A	6 degrees	2558 mm
B, J	16 degrees	2581 mm
D, K	26 degrees	2604 mm
G, N	29 degrees	2675 mm

The angle is measured relative to the 0° axis shown in Figure 2.
The radial position is relative to the axis of the reactor.

Table 8 Results for the Surveillance Capsules at 20°

Flux or Reaction	Cycle 5			Cycle 9			Cycle10		
	Calculated	Measured	C/M	Calculated	Measured	C/M	Calculated	Measured	C/M
ϕ>0.1MeV (n/cm^2.s)	1.31E11			7.05E10			5.10E10		
ϕ>1.0MeV (n/cm^2.s)	6.67E10			3.83E10			2.72E10		
dpa/s	9.7E-11			5.52E-11			3.93E-11		
	Activations at the time of measurement (dps/a)								
$Cu^{63}(n,\alpha)Co^{60}$	3.14E-17	3.63E-17	0.86	5.62E-18	5.89E-18	0.95	3.46E-17	3.92E-17	0.88
$Ti^{46}(n,p)Sc^{46}$	1.00E-16	9.85E-17	1.02	6.35E-16	6.60E-16	0.96	1.84E-16	1.88E-16	0.98
$Fe^{54}(n,p)Mn^{54}$	2.98E-15	2.80E-15	1.06	2.38E-15	1.97E-15	1.21	2.45E-15	2.22E-15	1.10
$Ni^{58}(n,p)Co^{58}$	4.63E-16	4.35E-16	1.06	4.71E-15	3.91E-15	1.21	1.11E-15	1.01E-15	1.10
$U^{238}(n,f)Cs^{137}$	3.04E-15	2.68E-15	1.13	3.23E-16	2.75E-16	1.17	4.66E-15		

Table 9 Power History

Cycle	Year	Month	Days	Mean Power
1	1971	12	31	0.0003
	1972	1	31	0.0827
		2	29	0.0095
		3	31	0.1314
		4	30	0.2855
		5	31	0.0000
		6	30	0.3759
		7	31	0.3557
		8	31	0.4211
		9	30	0.2693
		10	31	0.3884
		11	30	0.3031
		12	31	0.5692
	1973	1	31	0.3547
		2	28	0.0000
		3	31	0.5628
		4	30	0.8508
		5	31	0.5222
		6	30	0.8664
		7	31	0.8151
		8	31	0.2529
		9	30	0.0000
		10	31	0.0000
		11	30	0.0000
		12	31	0.0000
	1974	1	31	0.0000
		2	28	0.0000
		3	31	0.0000
		4	30	0.0000
		5	31	0.0000
		6	30	0.0000
		7	31	0.0000
		8	31	0.0000
		9	30	0.0000
		10	31	0.2056
		11	30	0.0046
		12	31	0.0000
	1975	1	31	0.0000
		2	28	0.0000
		3	31	0.0000
		4	30	0.5313
		5	31	0.7090
		6	30	0.4794
		7	31	0.5930
		8	31	0.3981
		9	30	0.5368
		10	31	0.6031
		11	30	0.6659
		12	20	0.4427
		12	11	0.0000
	1976	1	31	0.0000
		2	29	0.0000
		3	31	0.0000
		4	30	0.0000
		5	8	0.0000
2		5	23	0.4076
		6	30	0.8348
		7	31	0.5591
		8	31	0.6695
		9	30	0.7956
		10	31	0.6414
		11	30	0.5931
		12	31	0.8137
	1977	1	31	0.7578
		2	28	0.8404
		3	31	0.8007
		4	30	0.7987
		5	31	0.5444
		6	30	0.8762
		7	31	0.8259
		8	31	0.5965
		9	30	0.7858
		10	31	0.8661
		11	30	0.8003
		12	31	0.9051
	1978	1	31	0.1436
		1	25	0.0000
		2	28	0.0000
		3	31	0.0000
		4	19	0.0000
3		4	11	0.5713
		5	31	0.5033
		6	30	0.6836
		7	31	0.6844
		8	31	0.5573
		9	30	0.3052
		10	31	0.6229
		11	30	0.9240
		12	31	0.4511
	1979	1	31	0.9571
		2	28	0.9440
		3	31	0.9485
		4	30	0.7527
		5	31	0.3138
		6	30	0.7122
		7	31	0.9046

Note. The mean power is expressed as a fraction of 2530MW.

Table 9 Power History Continued

Cycle	Year	Month	Days	Mean Power
		8	31	0.8344
		9	8	0.6636
		9	22	0.0000
		10	31	0.0000
		11	30	0.0000
		12	31	0.0000
	1980	1	31	0.0000
		2	29	0.0000
		3	31	0.0000
		4	30	0.0000
		5	26	0.0000
4		5	5	0.5306
		6	30	0.8785
		7	31	0.6284
		8	31	0.7095
		9	30	0.7294
		10	31	0.8835
		11	30	0.0000
		12	31	0.4892
	1981	1	31	0.9445
		2	28	0.9906
		3	31	0.9919
		4	30	0.9608
		5	31	0.8720
		6	30	0.8408
		7	31	0.3211
		8	31	0.4493
		8	2	0.0000
		9	30	0.0000
		10	31	0.0000
		11	30	0.0000
		12	30	0.0000
5		12	1	0.0182
	1982	1	31	0.5036
		2	28	0.0990
		3	31	0.3624
		4	30	0.0000
		5	31	0.1925
		6	30	0.8862
		7	31	0.3090
		8	31	0.0000
		9	30	0.8558
		10	31	0.8870
		11	30	0.9896
		12	31	0.9783
	1983	1	31	0.9257
		2	28	0.9853
		3	31	0.9895
		4	30	0.9408
		5	31	0.8969
		6	30	0.9671
		7	31	0.9221
		8	12	0.7462
		8	19	0.0000
		9	30	0.0000
		10	31	0.0000
		11	30	0.0000
		12	31	0.0000
	1984	1	31	0.0000
		2	29	0.0000
		3	31	0.0000
		4	30	0.0000
		5	31	0.0000
		6	30	0.0000
		7	30	0.0000
6		7	1	0.1617
		8	31	0.0886
		9	30	0.1223
		10	31	0.0000
		11	30	0.2663
		12	31	0.9766
	1985	1	31	0.9576
		2	28	0.9190
		3	31	0.9794
		4	30	0.8908
		5	31	0.9782
		6	30	0.9377
		7	31	0.9687
		8	31	0.3405
		9	30	0.7537
		10	31	0.8273
		11	30	0.9575
		12	31	0.0000
	1986	1	31	0.0000
		2	28	0.0000
		3	3	0.0000
7		3	28	0.1949
		4	30	0.7257
		5	31	0.5883
		6	30	0.0000
		7	31	0.0000
		8	31	0.0000
		9	30	0.0000
		10	31	0.0000
		11	30	0.0000
		12	31	0.0000

Note. The mean power is expressed as a fraction of 2530MW.

Table 9 Power History Continued

Cycle	Year	Month	Days	Mean Power
	1987	1	31	0.0000
		2	28	0.0000
		3	31	0.0000
		4	30	0.5222
		5	31	0.7725
		6	30	0.7617
		7	31	0.4650
		8	31	0.7493
		9	30	0.8600
		10	31	0.0079
		11	30	0.5315
		12	31	0.1047
	1988	1	31	0.1087
		2	29	0.8433
		3	31	0.9979
		4	30	0.8357
		5	31	0.9198
		6	30	0.9984
		7	31	0.9532
		8	31	0.2363
		8	22	0.0000
		9	30	0.0000
		10	31	0.0000
		11	28	0.0000
8		11	2	0.2441
		12	31	0.2414
	1989	1	31	0.8808
		2	28	0.0000
		3	31	0.6631
		4	30	0.7642
		5	31	0.7967
		6	30	0.8002
		7	31	0.8027
		8	31	0.7129
		9	30	0.7978
		10	31	0.0003
		11	30	0.0000
		12	31	0.2668
	1990	1	31	0.7293
		2	28	0.7954
		3	31	0.7326
		4	30	0.4068
		5	31	0.2849
		6	30	0.5753
		7	31	0.7977
		8	31	0.7979
		9	15	0.7731
		9	15	0.0000

Cycle	Year	Month	Days	Mean Power
		10	31	0.0000
		11	30	0.0000
		12	31	0.0000
	1991	1	31	0.0000
		2	28	0.0000
		3	14	0.0000
9		3	17	0.4654
		4	30	0.9932
		5	31	1.0017
		6	30	0.9984
		7	31	0.6074
		8	31	0.9762
		9	30	0.9986
		10	31	1.0001
		11	30	0.9402
		12	31	0.8040
	1992	1	31	0.9920
		2	7	0.8420
		2	22	0.0000
		3	31	0.0000
		4	18	0.0000
10		4	12	0.8511
		5	31	0.9979
		6	30	0.9986
		7	31	0.7398
		8	31	0.7753
		9	30	0.6921
		10	31	0.9452
		11	30	0.7280
		12	31	0.9990
	1993	1	31	0.9985
		2	28	0.9990
		3	31	0.9991
		4	30	0.9272
		5	31	0.4583
		6	5	0.7835
		6	26	0.0000
		7	31	0.0000
		8	31	0.0000
		9	30	0.0000
		10	12	0.0000

Note. The mean power is expressed as a fraction of 2530MW.

Table 10 Calculated Spectral Response of the Monitors in the 20° Capsules

Det	Cycle	Group										
		2	3	4	5	6	7	8	9	10	11	12
		Lower Energy Limit (MeV)										
		13.5	12.0	10.0	7.79	6.07	3.68	2.87	2.23	1.74	1.35	0.82
		Percentage Contribution to the Reaction Rate										
Cu	5	1.8	2.6	8.9	27.7	38.4	20.3	0.3	0.0	0.0	0.0	0.0
	9	0.4	1.6	10.9	31.6	36.0	19.2	0.2	0.0	0.0	0.0	0.0
	10	0.0	4.5	6.5	31.0	35.8	21.8	0.2	0.0	0.0	0.0	0.0
Ti	5	0.6	0.9	3.7	15.4	32.6	44.9	1.7	0.0	0.0	0.0	0.0
	9	0.2	0.6	4.7	18.4	32.3	42.2	1.6	0.0	0.0	0.0	0.0
	10	0.0	1.5	2.6	17.1	31.0	46.3	1.5	0.0	0.0	0.0	0.0
Fe	5	0.1	0.3	1.2	5.8	17.3	48.9	14.3	9.0	2.6	0.4	0.1
	9	0.0	0.2	1.6	7.2	18.0	46.8	13.8	9.3	2.6	0.4	0.1
	10	0.0	0.4	0.8	6.6	17.4	51.8	12.5	7.5	2.5	0.4	0.1
Ni	5	0.1	0.2	1.1	5.8	16.9	45.1	13.7	11.0	3.8	1.6	0.6
	9	0.0	0.1	1.5	7.1	17.5	43.0	13.3	11.3	3.9	1.5	0.7
	10	0.0	0.4	0.8	6.6	17.0	48.0	12.0	9.2	3.7	1.5	0.6
U^{238}	5	0.2	0.2	0.7	3.5	9.1	22.4	12.2	19.8	17.2	12.8	2.0
	9	0.0	0.1	1.0	4.4	9.3	21.2	11.7	20.4	17.9	11.9	2.1
	10	0.0	0.3	0.5	4.2	9.2	24.9	11.1	17.4	18.2	12.1	2.0

Table 11 Fluxes and Decay Rates in the Capsules after Adjustments

Quantity	Initial Calculatd Value	Std Dev %	Measured Value	Std Dev %	Initial C/M	Std Dev %	Adjusted Calculatd Value	Std Dev %	C/M After Adjustment	Adj Factor
Cycle 5										
ϕ>0.1MeV(n/cm^2.s)	1.31E+11	10.1					1.22E+11	7.2		0.93
ϕ>1.0MeV(n/ cm^2.s)	6.67E+10	10.1					6.07E+10	7.2		0.91
dpa/s	9.70E-11	10.1					9.03E-11	5.5		0.93
Cu(n.p) Decay-Rate (dps/a)	3.14E-17	10.7	3.63E-17	5	0.86	11.8	3.41E-17	7.7	0.94	1.09
Ti(n.p) Decay - Rate (dps/a)	1.00E-16	10.4	9.85E-17	5	1.02	11.5	9.83E-17	7.4	1.03	0.98
Fe(n.p) Decay - Rate (dps/a)	2.98E-15	10.1	2.80E-15	5	1.06	11.3	2.81E-15	7.3	1.00	0.94
Ni(n.p) Decay - Rate (dps/a)	4.63E-16	10.1	4.35E-16	5	1.06	11.3	4.52E-16	7.3	1.00	0.98
U^{238}(n.f) Decay - Rate (dps/a)	3.04E-15	9.9	2.68E-15	5	1.13	11.1	2.77E-15	7.4	1.03	0.91
Cycle 9										
ϕ>0.1MeV(n/cm^2.s)	7.05E+10	10.2					6.37E+10	10.0		0.90
ϕ>1.0MeV(n/cm^2.s)	3.83E+10	10.2					3.27E+10	9.9		0.85
dpa/s	5.52E-11	10.0					4.73E-11	7.5		0.86
Cu(n.p) Decay - Rate (dps/a)	5.62E-18	10.5	5 89E-18	5	0.95	11.6	5.82E-18	10.7	0.98	1.04
Ti(n.p) Decay - Rate (dps/a)	6.35E-16	10.3	6.60E-16	5	0.96	11.4	6.13E-16	10.4	0.93	0.97
Fe(n.p) Decay - Rate (dps/a)	2.38E-15	10.0	1.97E-15	5	1.21	11.2	2.06E-15	10.5	1.05	0.87
Ni(n.p) Decay - Rate (dps/a)	4.71E-15	10.0	3.91E-15	5	1.21	11.2	4.08E-15	10.2	1.05	0.87
U^{238}(n.f) Decay - Rate (dps/a)	3.23E-16	10.0	2.75E-16	5	1.18	11.2	2.76E-16	10.2	1.01	0.85
Cycle 10										
ϕ>0.1MeV(n/cm^2.s)	5.10E+10	10.7					4.98E+10	8.8		0.98
ϕ>1.0MeV(n/cm^2.s)	2.72E+10	10.5					2.61E+10	9.2		0.96
dpa/s	3.93E-11	10.2					3.75E-11	6.7		0.95
Cu(n.p) Decay - Rate (dps/a)	3.46E-17	10.8	3.92E-17	5	0.88	11.9	3.77E-17	8.0	0.96	1.09
Ti(n.p) Decay - Rate (dps/a)	1.84E-16	10.1	1.88E-16	5	0.98	11.3	1.86E-16	7.7	0.99	1.01
Fe(n.p) Decay - Rate (dps/a)	2.45E-15	10.1	2.22E-15	5	1.1	11.3	2.29E-15	7.6	1.03	0.93
Ni(n.p) Decay - Rate (dps/a)	1.11E-15	10.1	1.01E-15	5	1.1	11.3	1.04E-15	7.4	1.03	0.94
U^{238}(n.f) Decay - Rate (dps/a)	4.66E-15	10.1								

Table 12 Calculated Reaction Rates and Fluxes for the 20° Capsules

Quantity	Cycles						
	1-4	5	6&7	8	9	10	11
Cu(n,a) (dps)	8.49E-17	9.90E-17	9.97E-17	8.00E-17	5.57E-17	4.07E-17	3.61E-17
Ti(n,p)) (dps)	1.40E-15	1.60E-15	1.57E-15	1.30E-15	9.16E-16	6.60E-16	5.79E-16
Fe(n,p)) (dps)	8.23E-15	9.15E-15	8.78E-15	7.50E-15	5.33E-15	3.79E-15	3.25E-15
Ni(n,p)) (dps)	1.07E-14	1.19E-14	1.14E-14	9.76E-15	6.88E-15	4.91E-15	4.19E-15
U^{238}(n,f)) (dps)	2.87E-14	2.99E-14	2.91E-14	2.50E-14	1.74E-14	1.25E-14	1.03E-14
f>0.1MeV ($n/cm^2.s$)	1.21E11	1.31E11	1.23E11	1.04E11	7.05E10	5.10E10	4.24E10
f>1.0Mev ($n/cm^2.s$)	6.45E10	6.67E10	6.36E10	5.51E10	3.83E10	2.72E10	2.21E10
Dpa rate (dpa/s)	9.12E-11	9.70E-11	9.01E-11	7.96E-11	5.52E-11	3.93E-11	3.25E-11
EFPS (secs)	1.30E08	3.41E7	6.07E7	3.23E7	2.58E7	3.08E7	3.72E7
Fluences							
Fluence E>0.1 MeV (n/cm^2)	1.57E19	4.47E18	7.47E18	3.36E18	1.82E18	1.57E18	1.58E18
Fluence E>1.0MeV (n/cm^2)	8.39E18	2.28E18	3.86E18	1.78E18	9.89E17	8.39E17	8.22E17
dpa	1.19E-2	3.31E-3	5.47E-3	2.57E-3	1.43E-3	1.21E-3	1.21E-3
Cumulative Values							
Fluence E>0.1 MeV (n/cm^2)	1.57E19	2.02E19	2.77E19	3.10E19	3.29E19	3.44E19	3.60E19
Fluence E>1.0MeV (n/cm^2)	8.39E18	1.07E19	1.45E19	1.63E19	1.73E19	1.81E19	1.90E19
(dpa)	1.19E-2	1.52E-2	2.06E-2	2.32E-2	2.46E-2	2.59E-2	2.71E-2
Adjusted Cumulative Values							
Fluence E>0.1 MeV (n/cm^2)	1.48E19	1.90E19	2.60E19	2.92E19	3.09E19	3.24E19	3.49E19
Fluence E>1.0MeV (n/cm^2)	7.64E18	9.71E18	1.32E19	1.48E19	1.57E19	1.65E19	1.73E19
(dpa)	1.08E-2	1.38E-2	1.88E-2	2.11E-2	2.24E-2	2.35E-2	2.46E-2

Note: The adjusted values have been multiplied by mean factors for the three capsules; i.e. 0.94 for ϕ>0.1MeV, and 0.91 for ϕ>1.0MeV and dpa.

Table 13 Calculated Axial Distributions of Fluences in the 20° Capsules

Distance from Core Centre Plane (cm)	Fluences Cycles 1 to 11		
	ϕ>0.1MeV n/cm^2	ϕ>1.0MeV n/cm^2	dpa
125 to 175	1.82E+19	9.61E+18	1.39E-02
75 to 125	3.17E+19	1.72E+19	2.44E-02
25 to 75	3.48E+19	1.88E+19	2.64E-02
-25 to 25	3.60E+19	1.90E+19	2.71E-02
-75 to -25	3.55E+19	1.91E+19	2.71E-02
-125 to -75	3.31E+19	1.78E+19	2.55E-02
-175 to -125	1.91E+19	1.01E+19	1.44E-02

Table 14 Calculated Fluxes and Decay Rates in the Cavity

Cycle			ϕ>0.1MeV	ϕ >1.0MeV	Cu(n,p)	Ti(n,p)	Fe(n,p)	Ni(n,p)	U238(n,f)	Np237(n,f)
8	Angle	16°	1.23E10	1.46E9	1.14E-19	4.56E-18	3.11E-17	3.25E-17	9.87E-18	1.51E-16
	Std Dv		1.0	2.0	3.5	2.6	1.9	1.7	1.9	1.2
	Angle	26°	1.09E10	1.09E9	1.01E-19	3.71E-18	2.46E-17	2.60E-17	7.71E-18	1.21E-16
	Std Dv		1.2	2.2	3.3	2.7	2.0	1.8	2.0	1.4
	Angle	39°	7.23E9	6.97E8	6.41E-20	2.27E-18	1.45E-17	1.55E-17	4.66E-18	7.62E-17
	Std Dv		1.3	3.1	3.8	3.0	2.5	2.4	3.5	1.7
9	Angle	16°	9.05E9	1.05E9	8.15E-20	8.11E-18	2.86E-17	6.14-17	5.97E-18	9.11E-17
	Std Dv		1.1	2.0	4.1	3.5	2.4	2.1	1.9	1.2
	Angle	26°	8.34E9	9.12E8	6.75E-20	6.67E-18	2.44E-17	5.24E-17	5.07E-18	7.88E-17
	Std Dv		1.7	2.3	4.1	3.6	2.7	2.5	2.1	1.7
	Angle	39°	5.98E9	5.97E8	4.29E-20	4.09E-18	1.49E-17	2.87E-17	3.26E-18	5.37E-17
	Std Dv		1.5	3.0	4.1	3.1	3.2	2.9	2.4	1.8
8&9	Angle	6°	4.87E9	5.67E8	1.65E-19	7.50E-18	3.64E-17	5.78E-17	1.44E-17	2.16E-16
	Std Dv		1.2	2.3	7.7	3.0	1.7	2.0	1.7	1.0

Note. The standard deviations are those arising solely from the Monte Carlo statistics and they are expressed as percentages.
The decay rates for the detectors are the calculated values at 12 December 1990 and 4 March 1992 for dosimetry removed after cycles 8 and 9 respectively.

Table 15 Values of C/M in the Cavity

Reaction	Cycle	Angle			6° Cycles 8 + 9
		16°	26°	39°	
Cu(n,a)	Cycle 8	1.01	1.16	1.00	1.15
	Cycle 9	1.15	1.11	1.02	
Ti(n,p)	Cycle 8	1.05	1.12	0.96	1.18
	Cycle 9	1.18	1.15	1.04	
Fe(n,p)	Cycle 8	1.17	1.23	1.01	1.30
	Cycle 9	1.29	1.29	1.18	
Ni(n,p)	Cycle 8	1.13	1.21	1.01	1.28
	Cycle 9	1.24	1.25	1.13	
U238(n,f)	Cycle 8	1.25	1.34	1.06	1.65
	Cycle 9	1.35	1.17	1.27	
Np237(n,f)	Cycle 8	0.98	1.06	0.94	1.35
	Cycle 9	1.25	1.14	1.31	

Table 16 Calculated Spectral Response of the Monitors in the Cavity for Cycle 8

Det	Angle	Group														
		3	4	5	6	7	8	9	10	11	12	13	14	15	16	17-30
		Lower Energy Limit (MeV)														
		12.0	10.0	7.79	6.07	3.68	2.87	2.23	1.74	1.35	0.82	0.50	0.30	0.18	0.068	0.0
		Percentage Contribution to the Reaction Rate														
Cu	16°	5.5	12.2	34.8	31.6	15.6	0.2									
	26°	2.7	13.2	38.6	30.5	14.6	0.3									
	39°	5.8	12.8	34.9	32.1	14.1	0.2									
Ti	16°	2.2	5.8	22.1	30.8	37.6	1.4									
	26°	1.1	6.5	24.0	30.0	36.5	1.8									
	39°	2.4	6.4	23.4	31.8	34.1	1.8									
Fe	16°	0.7	2.0	8.9	17.3	40.8	13.2	10.7	4.6	1.2	0.6					
	26°	0.2	2.2	9.2	16.8	40.1	13.9	11.0	4.9	1.1	0.6					
	39°	0.7	2.3	9.6	18.0	38.4	14.6	10.1	4.6	1.1	0.5					
Ni	16°	0.6	1.8	8.2	15.7	34.7	11.8	12.2	6.5	4.1	3.5	1.0				
	26°	0.2	2.0	8.5	15.2	34.2	12.5	12.5	6.7	3.7	3.5	1.0				
	39°	0.6	2.1	8.9	16.4	32.7	13.2	11.5	6.4	3.9	3.3	1.0				
U^{238}	16°	0.3	0.8	3.6	6.1	11.8	7.6	16.0	21.9	23.0	7.5	0.8	0.1			
	26°	0.2	0.9	3.8	5.8	12.2	7.8	16.6	23.1	20.7	7.6	0.9	0.1			
	39°	0.4	0.9	4.0	6.5	11.5	8.3	15.6	21.5	22.4	7.2	0.9	0.1	0.1	0.1	0.6
Np^{237}	16°	0.0	0.1	0.6	0.9	2.2	1.6	3.4	4.8	7.4	27.7	35.8	8.1	2.2	1.6	3.5
	26°	0.0	0.1	0.6	0.9	2.3	1.6	3.5	5.0	6.7	27.3	36.5	8.1	2.2	1.6	3.6
	39°	0.1	0.1	0.6	0.9	2.0	1.6	3.1	4.4	6.6	25.5	36.5	8.7	2.7	2.0	5.0

Table 17 Adjusted Fluxes and C/Ms in the Cavity

Cycle		ϕ>0.1MeV n/cm^2.s	ϕ >1.0MeV n/cm^2.s	dpa dps/a	Cu(n,p) C/M	Ti(n,p) C/M	Fe(n,p) C/M	Ni(n,p) C/M	U(n,f) C/M	Np(n,f) C/M
8	Adjustd	1.23E10	1.33E9	4.25E12	0.99	0.99	1.02	0.99	1.01	0.99
16°	Std Dv	7.3	5.0	5.5	4.7	4.6	4.6	4.5	7.5	8.4
	Initial	1.23E10	1.46E9	4.12E12	1.01	1.05	1.17	1.13	1.25	0.98
	Factor	1.00	0.91	0.97	0.98	0.94	0.87	0.88	0.81	1.01
8	Adjustd	1.06E10	9.26E8	3.42E12	1.02	0.97	1.02	1.00	1.01	1.00
26°	Std Dv	9.1	4.0	6.8	5.6	5.5	5.4	5.3	9.0	9.9
	Initial	1.09E10	1.09E9	3.64E12	1.16	1.12	1.23	1.21	1.34	1.06
	Factor	0.97	0.85	0.94	0.88	0.87	0.83	0.83	0.75	0.94
8	Adjustd	7.23E9	6.76E8	2.24E12	1.01	0.98	1.01	1.00	1.00	1.00
39°	Std Dv	4.3	5.9	3.8	2.2	2.2	2.1	2.1	3.5	6.6
	Initial	7.23E9	6.97E8	2.26E12	1.00	0.96	1.01	1.01	1.06	0.94
	Factor	1.0	0.96	0.99	1.01	1.02	1.01	0.99	0.94	1.06
9	Adjustd	8.05E9	8.82E8	2.66E12	1.00	0.99	1.02	0.99	1.01	1.01
16°	Std Dv	6.1	9.5	7.2	6.0	5.9	5.9	5.7	9.4	11.1
	Initial	9.05E9	1.05E9	3.06E12	1.15	1.18	1.29	1.24	1.35	1.25
	Factor	0.89	0.84	0.87	0.87	0.84	0.79	0.80	0.75	0.81
9	Adjustd	7.76E9	7.93E8	2.50E12	1.00	0.98	1.03	1.00	1.00	1.00
26°	Std Dv	9.2	4.6	6.9	5.6	5.7	5.6	5.4	8.5	10.4
	Initial	8.34E9	9.12E8	2.72E12	1.11	1.15	1.31	1.25	1.17	1.14
	Factor	0.93	0.87	0.92	0.90	0.85	0.79	0.80	0.85	0.88
9	Adjustd	5.28E9	4.66E8	1.70E12	1.00	0.99	1.03	0.98	1.01	1.01
39°	Std Dv	10.2	10.1	7.5	5.6	5.5	5.5	5.4	9.2	11.2
	Initial	5.98E9	5.97E8	1.97E12	1.02	1.04	1.18	1.33	1.27	1.31
	Factor	0.88	0.78	0.87	0.98	0.95	0.87	0.87	0.80	0.77

Note "Adjusted" = values of the parameters after adjustment by SENSAK.
"Std Dv" = percentage standard deviation assigned to the adjusted parameters by SENSAK.
"Initial" = values of the parameters before adjustment
"Factor" = factor by which the parameter has been changed by SENSAK.

Table 18 Cycles 1 to 4 Combined, Flux>0.1MeV in Vessel Wall at Mid-height

Angle from Vertical	Distance Through Vessel Wall (T is wall thickness)				
	Inner Edge	T/4	T/2	3T/4	Outer Edge
0° to 5°	7.41E+10	6.05E+10	4.38E+10	2.96E+10	1.64E+10
5° to 10°	8.32E+10	6.64E+10	4.86E+10	3.25E+10	1.81E+10
10° to 15°	9.48E+10	7.67E+10	5.50E+10	3.57E+10	1.99E+10
15° to 20°	9.88E+10	7.90E+10	5.55E+10	3.66E+10	2.01E+10
20° to 25°	8.49E+10	6.69E+10	4.91E+10	3.28E+10	1.82E+10
25° to 30°	7.30E+10	6.06E+10	4.44E+10	2.91E+10	1.63E+10
30° to 35°	7.51E+10	5.97E+10	4.34E+10	2.87E+10	1.63E+10
35° to 40°	6.47E+10	5.26E+10	3.77E+10	2.53E+10	1.46E+10
40° to 45°	5.04E+10	4.20E+10	3.07E+10	2.14E+10	1.27E+10
45° to 50°	4.93E+10	4.04E+10	3.11E+10	2.17E+10	1.36E+10
50° to 55°	6.64E+10	5.23E+10	3.72E+10	2.60E+10	1.53E+10
55° to 60°	7.88E+10	6.22E+10	4.42E+10	2.89E+10	1.67E+10
60° to 65°	7.66E+10	6.24E+10	4.45E+10	3.01E+10	1.71E+10
65° to 70°	8.16E+10	6.91E+10	4.93E+10	3.32E+10	1.85E+10
70° to 75°	9.91E+10	7.81E+10	5.55E+10	3.65E+10	1.99E+10
75° to 80°	9.63E+10	7.55E+10	5.42E+10	3.54E+10	1.97E+10
80° to 85°	8.00E+10	6.58E+10	4.76E+10	3.19E+10	1.84E+10
85° to 90°	7.53E+10	6.14E+10	4.39E+10	2.93E+10	1.68E+10

Table 19 Cycle 5, Flux>0.1MeV in Vessel Wall at Mid-height

Angle from Vertical	Distance Through Vessel Wall (T is wall thickness)				
	Inner Edge	T/4	T/2	3T/4	Outer Edge
0° to 5°	7.96E+10	6.41E+10	4.83E+10	3.21E+10	1.93E+10
5° to 10°	8.80E+10	7.10E+10	5.22E+10	3.49E+10	2.03E+10
10° to 15°	1.04E+11	8.51E+10	6.00E+10	3.89E+10	2.16E+10
15° to 20°	1.11E+11	8.71E+10	6.20E+10	4.05E+10	2.24E+10
20° to 25°	9.50E+10	7.66E+10	5.53E+10	3.69E+10	2.09E+10
25° to 30°	8.63E+10	6.89E+10	4.95E+10	3.34E+10	1.93E+10
30° to 35°	8.58E+10	6.85E+10	4.88E+10	3.24E+10	1.89E+10
35° to 40°	7.33E+10	6.08E+10	4.39E+10	2.93E+10	1.70E+10
40° to 45°	5.47E+10	4.62E+10	3.43E+10	2.43E+10	1.48E+10
45° to 50°	5.52E+10	4.71E+10	3.46E+10	2.46E+10	1.54E+10
50° to 55°	7.47E+10	6.01E+10	4.34E+10	2.93E+10	1.67E+10
55° to 60°	8.57E+10	6.84E+10	4.92E+10	3.35E+10	1.90E+10
60° to 65°	8.84E+10	7.29E+10	5.26E+10	3.50E+10	2.01E+10
65° to 70°	9.86E+10	7.92E+10	5.71E+10	3.76E+10	2.10E+10
70° to 75°	1.09E+11	8.62E+10	6.10E+10	4.01E+10	2.14E+10
75° to 80°	1.03E+11	8.41E+10	5.90E+10	3.89E+10	2.17E+10
80° to 85°	9.18E+10	7.38E+10	5.38E+10	3.53E+10	1.98E+10
85° to 90°	7.71E+10	6.55E+10	4.67E+10	3.18E+10	1.82E+10

Table 20 Cycles 6 and 7 Combined, Flux>0.1MeV in Vessel Wall at Mid-height

Angle from Vertical	Distance Through Vessel Wall (T is wall thickness)				
	Inner Edge	T/4	T/2	3T/4	Outer Edge
0° to 5°	8.61E+10	7.02E+10	5.18E+10	3.53E+10	2.02E+10
5° to 10°	8.99E+10	7.42E+10	5.51E+10	3.70E+10	2.08E+10
10° to 15°	1.04E+11	8.21E+10	5.96E+10	3.93E+10	2.18E+10
15° to 20°	1.04E+11	8.24E+10	6.08E+10	3.85E+10	2.10E+10
20° to 25°	9.46E+10	7.88E+10	5.47E+10	3.75E+10	2.03E+10
25° to 30°	8.73E+10	7.18E+10	5.26E+10	3.54E+10	1.98E+10
30° to 35°	8.50E+10	6.82E+10	4.73E+10	3.13E+10	1.83E+10
35° to 40°	7.44E+10	5.80E+10	4.32E+10	2.85E+10	1.64E+10
40° to 45°	5.53E+10	4.62E+10	3.52E+10	2.40E+10	1.48E+10
45° to 50°	5.19E+10	4.65E+10	3.39E+10	2.34E+10	1.45E+10
50° to 55°	7.21E+10	5.90E+10	4.14E+10	2.82E+10	1.67E+10
55° to 60°	8.62E+10	6.88E+10	4.90E+10	3.29E+10	1.83E+10
60° to 65°	8.18E+10	6.62E+10	4.78E+10	3.37E+10	1.93E+10
65° to 70°	9.60E+10	7.56E+10	5.26E+10	3.57E+10	2.05E+10
70° to 75°	1.08E+11	8.62E+10	6.01E+10	4.01E+10	2.20E+10
75° to 80°	1.11E+11	8.88E+10	6.32E+10	4.12E+10	2.19E+10
80° to 85°	9.22E+10	7.51E+10	5.44E+10	3.65E+10	2.03E+10
85° to 90°	9.12E+10	6.96E+10	5.11E+10	3.42E+10	1.91E+10

Table 21 Cycle 8, Flux>0.1MeV in Vessel Wall at Mid-height

Angle from Vertical	Distance Through Vessel Wall (T is wall thickness)				
	Inner Edge	T/4	T/2	3T/4	Outer Edge
0° to 5°	4.31E+10	3.74E+10	2.82E+10	1.95E+10	1.16E+10
5° to 10°	6.30E+10	4.99E+10	3.64E+10	2.43E+10	1.36E+10
10° to 15°	8.54E+10	6.67E+10	4.74E+10	3.11E+10	1.64E+10
15° to 20°	9.12E+10	7.29E+10	5.06E+10	3.27E+10	1.70E+10
20° to 25°	7.31E+10	5.86E+10	4.13E+10	2.72E+10	1.44E+10
25° to 30°	5.06E+10	4.13E+10	2.93E+10	2.03E+10	1.13E+10
30° to 35°	3.65E+10	3.06E+10	2.25E+10	1.58E+10	9.51E+09
35° to 40°	3.19E+10	2.64E+10	1.94E+10	1.38E+10	8.43E+09
40° to 45°	2.93E+10	2.39E+10	1.78E+10	1.24E+10	7.81E+09
45° to 50°	2.90E+10	2.39E+10	1.74E+10	1.23E+10	7.86E+09
50° to 55°	3.16E+10	2.59E+10	1.93E+10	1.35E+10	8.38E+09
55° to 60°	3.65E+10	3.04E+10	2.24E+10	1.55E+10	9.57E+09
60° to 65°	5.13E+10	4.04E+10	2.96E+10	1.99E+10	1.17E+10
65° to 70°	7.18E+10	5.70E+10	4.11E+10	2.70E+10	1.46E+10
70° to 75°	9.26E+10	7.24E+10	5.00E+10	3.21E+10	1.69E+10
75° to 80°	8.45E+10	6.77E+10	4.68E+10	3.02E+10	1.60E+10
80° to 85°	5.99E+10	4.95E+10	3.51E+10	2.36E+10	1.30E+10
85° to 90°	4.26E+10	3.66E+10	2.73E+10	1.87E+10	1.12E+10

Table 22 Cycle 9, Flux>0.1MeV in Vessel Wall at Mid-height

Angle from Vertical	Distance Through Vessel Wall (T is wall thickness)				
	Inner Edge	T/4	T/2	3T/4	Outer Edge
0° to 5°	3.98E+10	3.39E+10	2.47E+10	1.67E+10	9.78E+09
5° to 10°	4.79E+10	3.73E+10	2.74E+10	1.88E+10	1.05E+10
10° to 15°	5.48E+10	4.47E+10	3.20E+10	2.15E+10	1.15E+10
15° to 20°	6.01E+10	4.68E+10	3.34E+10	2.20E+10	1.15E+10
20° to 25°	5.19E+10	4.07E+10	3.00E+10	1.98E+10	1.11E+10
25° to 30°	4.22E+10	3.49E+10	2.49E+10	1.67E+10	9.52E+09
30° to 35°	3.55E+10	2.84E+10	2.08E+10	1.41E+10	8.15E+09
35° to 40°	2.94E+10	2.38E+10	1.73E+10	1.20E+10	7.37E+09
40° to 45°	2.23E+10	1.92E+10	1.41E+10	1.03E+10	6.37E+09
45° to 50°	2.19E+10	1.87E+10	1.38E+10	9.87E+09	6.43E+09
50° to 55°	2.74E+10	2.28E+10	1.65E+10	1.15E+10	7.02E+09
55° to 60°	3.50E+10	2.86E+10	2.05E+10	1.37E+10	8.12E+09
60° to 65°	4.30E+10	3.48E+10	2.44E+10	1.63E+10	9.33E+09
65° to 70°	4.99E+10	3.87E+10	2.83E+10	1.93E+10	1.03E+10
70° to 75°	5.80E+10	4.61E+10	3.27E+10	2.14E+10	1.14E+10
75° to 80°	5.54E+10	4.44E+10	3.16E+10	2.08E+10	1.14E+10
80° to 85°	4.62E+10	3.80E+10	2.75E+10	1.88E+10	1.07E+10
85° to 90°	4.13E+10	3.36E+10	2.49E+10	1.66E+10	9.73E+09

Table 23 Cycle 10, Flux>0.1MeV in Vessel Wall at Mid-height

Angle from Vertical	Distance Through Vessel Wall (T is wall thickness)				
	Inner Edge	T/4	T/2	3T/4	Outer Edge
0° to 5°	3.12E+10	2.55E+10	1.85E+10	1.29E+10	7.86E+09
5° to 10°	3.54E+10	2.91E+10	2.12E+10	1.43E+10	8.12E+09
10° to 15°	4.32E+10	3.43E+10	2.48E+10	1.63E+10	8.80E+09
15° to 20°	4.52E+10	3.51E+10	2.52E+10	1.67E+10	8.90E+09
20° to 25°	4.11E+10	3.30E+10	2.36E+10	1.56E+10	8.72E+09
25° to 30°	3.93E+10	3.16E+10	2.20E+10	1.46E+10	8.22E+09
30° to 35°	3.50E+10	2.84E+10	2.05E+10	1.36E+10	7.56E+09
35° to 40°	2.91E+10	2.36E+10	1.75E+10	1.19E+10	6.92E+09
40° to 45°	2.37E+10	2.05E+10	1.55E+10	1.07E+10	6.36E+09
45° to 50°	2.58E+10	2.14E+10	1.56E+10	1.08E+10	6.37E+09
50° to 55°	3.00E+10	2.45E+10	1.81E+10	1.22E+10	7.04E+09
55° to 60°	3.49E+10	2.78E+10	2.01E+10	1.31E+10	7.42E+09
60° to 65°	3.68E+10	3.04E+10	2.12E+10	1.42E+10	8.20E+09
65° to 70°	3.96E+10	3.27E+10	2.38E+10	1.61E+10	8.86E+09
70° to 75°	4.41E+10	3.54E+10	2.54E+10	1.64E+10	9.01E+09
75° to 80°	4.20E+10	3.32E+10	2.42E+10	1.58E+10	8.90E+09
80° to 85°	3.52E+10	2.95E+10	2.12E+10	1.41E+10	7.79E+09
85° to 90°	2.89E+10	2.45E+10	1.80E+10	1.26E+10	7.32E+09

Table 24 Cycle 11, Flux>0.1MeV in Vessel Wall at Mid-height

Angle from Vertical	Distance Through Vessel Wall (T is wall thickness)				
	Inner Edge	T/4	T/2	3T/4	Outer Edge
0° to 5°	2.71E+10	2.19E+10	1.58E+10	1.11E+10	6.40E+09
5° to 10°	3.16E+10	2.51E+10	1.81E+10	1.25E+10	6.91E+09
10° to 15°	3.55E+10	2.82E+10	2.00E+10	1.30E+10	7.45E+09
15° to 20°	3.54E+10	2.86E+10	2.05E+10	1.34E+10	7.47E+09
20° to 25°	3.24E+10	2.53E+10	1.88E+10	1.25E+10	7.13E+09
25° to 30°	2.89E+10	2.48E+10	1.77E+10	1.18E+10	7.01E+09
30° to 35°	2.82E+10	2.32E+10	1.68E+10	1.09E+10	6.33E+09
35° to 40°	2.28E+10	1.92E+10	1.39E+10	9.54E+09	5.63E+09
40° to 45°	1.93E+10	1.65E+10	1.21E+10	8.67E+09	5.34E+09
45° to 50°	1.99E+10	1.64E+10	1.20E+10	8.54E+09	5.21E+09
50° to 55°	2.50E+10	1.97E+10	1.42E+10	9.60E+09	5.72E+09
55° to 60°	2.84E+10	2.30E+10	1.66E+10	1.11E+10	6.47E+09
60° to 65°	3.06E+10	2.43E+10	1.81E+10	1.19E+10	6.91E+09
65° to 70°	3.22E+10	2.74E+10	2.00E+10	1.32E+10	7.42E+09
70° to 75°	4.00E+10	3.13E+10	2.17E+10	1.45E+10	7.86E+09
75° to 80°	4.03E+10	3.27E+10	2.23E+10	1.49E+10	8.11E+09
80° to 85°	3.32E+10	2.72E+10	1.95E+10	1.31E+10	7.46E+09
85° to 90°	2.69E+10	2.21E+10	1.65E+10	1.13E+10	6.71E+09

Table 25 Cycles 1 to 4 Combined. Flux>1.0MeV in Vessel Wall at Mid-height

Angle from Vertical	Distance Through Vessel Wall (T is wall thickness)				
	Inner Edge	T/4	T/2	3T/4	Outer Edge
0° to 5°	3.33E+10	1.90E+10	9.72E+09	4.44E+09	1.79E+09
5° to 10°	3.79E+10	2.06E+10	1.05E+10	4.87E+09	2.03E+09
10° to 15°	4.48E+10	2.43E+10	1.22E+10	5.49E+09	2.28E+09
15° to 20°	4.57E+10	2.45E+10	1.15E+10	5.53E+09	2.19E+09
20° to 25°	3.88E+10	2.08E+10	1.04E+10	4.82E+09	1.95E+09
25° to 30°	3.26E+10	1.81E+10	8.97E+09	4.19E+09	1.78E+09
30° to 35°	3.39E+10	1.87E+10	8.94E+09	4.17E+09	1.78E+09
35° to 40°	2.91E+10	1.61E+10	7.67E+09	3.54E+09	1.50E+09
40° to 45°	2.28E+10	1.29E+10	6.29E+09	3.07E+09	1.32E+09
45° to 50°	2.24E+10	1.22E+10	6.24E+09	2.93E+09	1.31E+09
50° to 55°	3.03E+10	1.62E+10	7.89E+09	3.78E+09	1.56E+09
55° to 60°	3.57E+10	1.96E+10	9.55E+09	4.39E+09	1.83E+09
60° to 65°	3.62E+10	1.96E+10	9.42E+09	4.21E+09	1.81E+09
65° to 70°	3.74E+10	2.12E+10	1.04E+10	4.93E+09	2.01E+09
70° to 75°	4.58E+10	2.46E+10	1.18E+10	5.41E+09	2.17E+09
75° to 80°	4.40E+10	2.38E+10	1.18E+10	5.54E+09	2.24E+09
80° to 85°	3.66E+10	2.02E+10	9.88E+09	4.67E+09	1.93E+09
85° to 90°	3.49E+10	1.88E+10	9.18E+09	4.36E+09	1.79E+09

Table 26 Cycle 5, Flux>1.0MeV in Vessel Wall at Mid-height

Angle from Vertical	Distance Through Vessel Wall (T is wall thickness)				
	Inner Edge	T/4	T/2	3T/4	Outer Edge
0° to 5°	3.70E+10	1.94E+10	9.85E+09	4.57E+09	1.93E+09
5° to 10°	3.95E+10	2.17E+10	1.07E+10	4.91E+09	2.06E+09
10° to 15°	4.85E+10	2.61E+10	1.27E+10	5.71E+09	2.36E+09
15° to 20°	5.01E+10	2.70E+10	1.30E+10	6.14E+09	2.52E+09
20° to 25°	4.43E+10	2.38E+10	1.18E+10	5.48E+09	2.32E+09
25° to 30°	3.87E+10	2.07E+10	1.03E+10	4.84E+09	2.02E+09
30° to 35°	3.90E+10	2.10E+10	1.06E+10	4.84E+09	2.01E+09
35° to 40°	3.36E+10	1.85E+10	9.06E+09	4.14E+09	1.78E+09
40° to 45°	2.51E+10	1.37E+10	7.01E+09	3.29E+09	1.43E+09
45° to 50°	2.54E+10	1.36E+10	7.04E+09	3.33E+09	1.43E+09
50° to 55°	3.42E+10	1.84E+10	9.06E+09	4.26E+09	1.80E+09
55° to 60°	4.01E+10	2.12E+10	1.04E+10	4.91E+09	1.98E+09
60° to 65°	4.04E+10	2.13E+10	1.09E+10	4.94E+09	2.09E+09
65° to 70°	4.40E+10	2.39E+10	1.18E+10	5.23E+09	2.20E+09
70° to 75°	5.00E+10	2.67E+10	1.28E+10	6.13E+09	2.43E+09
75° to 80°	4.70E+10	2.62E+10	1.24E+10	5.91E+09	2.27E+09
80° to 85°	4.19E+10	2.29E+10	1.12E+10	4.95E+09	2.26E+09
85° to 90°	3.59E+10	1.99E+10	9.57E+09	4.68E+09	1.91E+09

Table 27 Cycles 6 and 7 Combined, Flux>1.0MeV in Vessel Wall at Mid-height

Angle from Vertical	Distance Through Vessel Wall (T is wall thickness)				
	Inner Edge	T/4	T/2	3T/4	Outer Edge
0° to 5°	4.02E+10	2.23E+10	1.13E+10	5.13E+09	2.20E+09
5° to 10°	4.43E+10	2.39E+10	1.16E+10	5.55E+09	2.32E+09
10° to 15°	4.96E+10	2.61E+10	1.28E+10	6.07E+09	2.52E+09
15° to 20°	4.86E+10	2.58E+10	1.29E+10	5.64E+09	2.33E+09
20° to 25°	4.31E+10	2.31E+10	1.12E+10	5.09E+09	1.99E+09
25° to 30°	3.88E+10	2.13E+10	1.06E+10	5.26E+09	2.13E+09
30° to 35°	3.90E+10	2.07E+10	1.00E+10	4.59E+09	1.93E+09
35° to 40°	3.42E+10	1.83E+10	9.01E+09	4.13E+09	1.76E+09
40° to 45°	2.40E+10	1.32E+10	6.79E+09	3.11E+09	1.46E+09
45° to 50°	2.39E+10	1.39E+10	6.55E+09	3.22E+09	1.44E+09
50° to 55°	3.19E+10	1.85E+10	8.48E+09	4.04E+09	1.71E+09
55° to 60°	3.94E+10	2.14E+10	1.05E+10	4.91E+09	1.95E+09
60° to 65°	3.93E+10	2.03E+10	9.79E+09	4.91E+09	2.01E+09
65° to 70°	4.37E+10	2.21E+10	1.07E+10	5.27E+09	2.14E+09
70° to 75°	4.92E+10	2.72E+10	1.29E+10	6.17E+09	2.46E+09
75° to 80°	5.03E+10	2.75E+10	1.33E+10	6.13E+09	2.43E+09
80° to 85°	4.32E+10	2.38E+10	1.14E+10	5.15E+09	2.29E+09
85° to 90°	3.98E+10	2.10E+10	1.00E+10	5.00E+09	2.00E+09

Table 28 Cycle 8, Flux>1.0MeV in Vessel Wall at Mid-height

Angle from Vertical	Distance Through Vessel Wall (T is wall thickness)				
	Inner Edge	T/4	T/2	3T/4	Outer Edge
0° to 5°	1.94E+10	1.11E+10	5.34E+09	2.57E+09	1.13E+09
5° to 10°	2.86E+10	1.51E+10	7.40E+09	3.51E+09	1.48E+09
10° to 15°	3.95E+10	2.11E+10	1.02E+10	4.75E+09	1.89E+09
15° to 20°	4.22E+10	2.32E+10	1.09E+10	5.08E+09	1.99E+09
20° to 25°	3.25E+10	1.77E+10	8.63E+09	3.98E+09	1.63E+09
25° to 30°	2.30E+10	1.24E+10	5.98E+09	2.84E+09	1.19E+09
30° to 35°	1.68E+10	9.38E+09	4.58E+09	2.25E+09	8.86E+08
35° to 40°	1.50E+10	8.00E+09	4.06E+09	1.86E+09	8.50E+08
40° to 45°	1.37E+10	7.48E+09	3.73E+09	1.72E+09	7.95E+08
45° to 50°	1.35E+10	7.30E+09	3.43E+09	1.69E+09	7.51E+08
50° to 55°	1.48E+10	7.70E+09	3.86E+09	1.80E+09	8.03E+08
55° to 60°	1.65E+10	9.17E+09	4.43E+09	2.13E+09	9.09E+08
60° to 65°	2.31E+10	1.23E+10	6.03E+09	2.85E+09	1.22E+09
65° to 70°	3.31E+10	1.77E+10	8.76E+09	4.18E+09	1.69E+09
70° to 75°	4.28E+10	2.30E+10	1.11E+10	5.18E+09	2.07E+09
75° to 80°	4.01E+10	2.14E+10	1.04E+10	4.84E+09	1.99E+09
80° to 85°	2.80E+10	1.53E+10	7.50E+09	3.59E+09	1.45E+09
85° to 90°	1.99E+10	1.09E+10	5.37E+09	2.61E+09	1.17E+09

Table 29 Cycle 9, Flux>1.0MeV in Vessel Wall at Mid-height

Angle from Vertical	Distance Through Vessel Wall (T is wall thickness)				
	Inner Edge	T/4	T/2	3T/4	Outer Edge
0° to 5°	1.82E+10	1.03E+10	5.17E+09	2.43E+09	1.01E+09
5° to 10°	2.24E+10	1.17E+10	5.80E+09	2.80E+09	1.19E+09
10° to 15°	2.62E+10	1.41E+10	6.93E+09	3.32E+09	1.32E+09
15° to 20°	2.77E+10	1.47E+10	7.10E+09	3.32E+09	1.32E+09
20° to 25°	2.40E+10	1.26E+10	6.14E+09	2.98E+09	1.23E+09
25° to 30°	1.94E+10	1.07E+10	5.14E+09	2.45E+09	1.04E+09
30° to 35°	1.63E+10	8.79E+09	4.38E+09	2.04E+09	8.65E+08
35° to 40°	1.32E+10	7.43E+09	3.67E+09	1.73E+09	7.63E+08
40° to 45°	1.01E+10	5.70E+09	2.84E+09	1.39E+09	6.28E+08
45° to 50°	1.03E+10	5.63E+09	2.88E+09	1.37E+09	6.17E+08
50° to 55°	1.24E+10	6.90E+09	3.43E+09	1.61E+09	7.44E+08
55° to 60°	1.63E+10	8.82E+09	4.27E+09	2.03E+09	8.48E+08
60° to 65°	1.95E+10	1.05E+10	5.12E+09	2.39E+09	1.04E+09
65° to 70°	2.32E+10	1.27E+10	6.15E+09	2.95E+09	1.24E+09
70° to 75°	2.71E+10	1.47E+10	7.19E+09	3.31E+09	1.28E+09
75° to 80°	2.59E+10	1.40E+10	6.83E+09	3.11E+09	1.30E+09
80° to 85°	2.13E+10	1.18E+10	5.75E+09	2.74E+09	1.17E+09
85° to 90°	1.89E+10	1.02E+10	5.08E+09	2.40E+09	1.08E+09

Table 30 Cycle10, Flux>1.0MeV in Vessel Wall at Mid-height

Angle from Vertical	Distance Through Vessel Wall (T is wall thickness)				
	Inner Edge	T/4	T/2	3T/4	Outer Edge
0° to 5°	1.43E+10	7.62E+09	3.95E+09	1.82E+09	8.14E+08
5° to 10°	1.62E+10	8.84E+09	4.61E+09	2.16E+09	8.62E+08
10° to 15°	1.98E+10	1.09E+10	5.45E+09	2.40E+09	9.59E+08
15° to 20°	2.00E+10	1.09E+10	5.46E+09	2.60E+09	1.06E+09
20° to 25°	1.87E+10	1.02E+10	4.87E+09	2.33E+09	9.26E+08
25° to 30°	1.77E+10	9.94E+09	4.87E+09	2.16E+09	9.31E+08
30° to 35°	1.61E+10	9.03E+09	4.45E+09	2.11E+09	9.01E+08
35° to 40°	1.37E+10	7.28E+09	3.63E+09	1.68E+09	7.00E+08
40° to 45°	1.09E+10	6.31E+09	3.05E+09	1.57E+09	6.60E+08
45° to 50°	1.17E+10	6.57E+09	3.13E+09	1.45E+09	6.51E+08
50° to 55°	1.34E+10	7.57E+09	3.72E+09	1.72E+09	7.34E+08
55° to 60°	1.64E+10	8.75E+09	4.21E+09	1.97E+09	8.35E+08
60° to 65°	1.72E+10	9.45E+09	4.55E+09	2.24E+09	9.37E+08
65° to 70°	1.81E+10	1.01E+10	4.85E+09	2.30E+09	9.14E+08
70° to 75°	2.00E+10	1.07E+10	5.37E+09	2.53E+09	1.03E+09
75° to 80°	1.99E+10	1.02E+10	5.09E+09	2.45E+09	9.78E+08
80° to 85°	1.62E+10	9.25E+09	4.52E+09	2.15E+09	8.64E+08
85° to 90°	1.34E+10	7.38E+09	3.72E+09	1.81E+09	7.76E+08

Table 31 Cycle 11, Flux>1.0MeV in Vessel Wall at Mid-height

Angle from Vertical	Distance Through Vessel Wall (T is wall thickness)				
	Inner Edge	T/4	T/2	3T/4	Outer Edge
0° to 5°	1.31E+10	6.97E+09	3.39E+09	1.68E+09	6.83E+08
5° to 10°	1.51E+10	7.96E+09	3.92E+09	1.81E+09	7.38E+08
10° to 15°	1.68E+10	8.95E+09	4.35E+09	1.91E+09	8.39E+08
15° to 20°	1.64E+10	8.85E+09	4.36E+09	1.99E+09	8.63E+08
20° to 25°	1.44E+10	7.64E+09	3.74E+09	1.79E+09	7.70E+08
25° to 30°	1.34E+10	7.63E+09	3.67E+09	1.70E+09	7.44E+08
30° to 35°	1.32E+10	7.27E+09	3.53E+09	1.62E+09	6.31E+08
35° to 40°	1.09E+10	6.15E+09	2.88E+09	1.33E+09	5.79E+08
40° to 45°	8.92E+09	5.00E+09	2.55E+09	1.16E+09	5.34E+08
45° to 50°	9.21E+09	4.99E+09	2.51E+09	1.19E+09	5.25E+08
50° to 55°	1.16E+10	6.15E+09	2.97E+09	1.39E+09	5.82E+08
55° to 60°	1.32E+10	7.30E+09	3.58E+09	1.72E+09	6.84E+08
60° to 65°	1.46E+10	7.52E+09	3.88E+09	1.86E+09	7.72E+08
65° to 70°	1.50E+10	8.51E+09	4.07E+09	1.86E+09	7.90E+08
70° to 75°	1.89E+10	9.73E+09	4.81E+09	2.24E+09	9.54E+08
75° to 80°	1.87E+10	1.01E+10	4.72E+09	2.26E+09	9.12E+08
80° to 85°	1.54E+10	8.24E+09	4.12E+09	2.05E+09	8.30E+08
85° to 90°	1.26E+10	6.94E+09	3.48E+09	1.67E+09	7.22E+08

Table 32 Cycles 1 to 4 Combined, dpa/s in Vessel Wall at Mid-height

Angle from Vertical	Distance Through Vessel Wall (T is wall thickness)				
	Inner Edge	T/4	T/2	3T/4	Outer Edge
0° to 5°	4.99E-11	3.04E-11	1.80E-11	1.04E-11	5.18E-12
5° to 10°	5.64E-11	3.32E-11	1.99E-11	1.14E-11	5.83E-12
10° to 15°	6.52E-11	3.89E-11	2.26E-11	1.27E-11	6.38E-12
15° to 20°	6.65E-11	3.94E-11	2.24E-11	1.29E-11	6.39E-12
20° to 25°	5.68E-11	3.36E-11	1.97E-11	1.14E-11	5.77E-12
25° to 30°	4.87E-11	2.97E-11	1.77E-11	1.00E-11	5.19E-12
30° to 35°	5.01E-11	2.98E-11	1.74E-11	9.86E-12	5.15E-12
35° to 40°	4.39E-11	2.62E-11	1.51E-11	8.72E-12	4.54E-12
40° to 45°	3.38E-11	2.08E-11	1.23E-11	7.39E-12	4.01E-12
45° to 50°	3.34E-11	2.02E-11	1.24E-11	7.40E-12	4.15E-12
50° to 55°	4.45E-11	2.61E-11	1.51E-11	8.99E-12	4.80E-12
55° to 60°	5.29E-11	3.13E-11	1.81E-11	1.02E-11	5.33E-12
60° to 65°	5.24E-11	3.11E-11	1.80E-11	1.04E-11	5.42E-12
65° to 70°	5.60E-11	3.45E-11	2.00E-11	1.16E-11	5.91E-12
70° to 75°	6.71E-11	3.93E-11	2.26E-11	1.29E-11	6.31E-12
75° to 80°	6.49E-11	3.82E-11	2.23E-11	1.26E-11	6.35E-12
80° to 85°	5.52E-11	3.35E-11	1.95E-11	1.12E-11	5.83E-12
85° to 90°	5.19E-11	3.10E-11	1.80E-11	1.03E-11	5.33E-12

Table 33 Cycle 5, dpa/s in Vessel Wall at Mid-height

Angle from Vertical	Distance Through Vessel Wall (T is wall thickness)				
	Inner Edge	T/4	T/2	3T/4	Outer Edge
0° to 5°	5.47E-11	3.20E-11	1.93E-11	1.11E-11	5.93E-12
5° to 10°	5.92E-11	3.55E-11	2.11E-11	1.21E-11	6.33E-12
10° to 15°	7.09E-11	4.23E-11	2.42E-11	1.35E-11	6.83E-12
15° to 20°	7.41E-11	4.33E-11	2.51E-11	1.42E-11	7.12E-12
20° to 25°	6.44E-11	3.84E-11	2.27E-11	1.30E-11	6.60E-12
25° to 30°	5.73E-11	3.47E-11	2.02E-11	1.17E-11	6.14E-12
30° to 35°	5.78E-11	3.39E-11	1.97E-11	1.14E-11	5.96E-12
35° to 40°	4.98E-11	3.03E-11	1.76E-11	1.01E-11	5.36E-12
40° to 45°	3.74E-11	2.29E-11	1.37E-11	8.29E-12	4.60E-12
45° to 50°	3.79E-11	2.30E-11	1.38E-11	8.31E-12	4.77E-12
50° to 55°	5.03E-11	3.00E-11	1.74E-11	1.01E-11	5.32E-12
55° to 60°	5.83E-11	3.44E-11	2.00E-11	1.16E-11	5.95E-12
60° to 65°	6.01E-11	3.59E-11	2.11E-11	1.21E-11	6.37E-12
65° to 70°	6.57E-11	3.95E-11	2.31E-11	1.30E-11	6.60E-12
70° to 75°	7.33E-11	4.33E-11	2.48E-11	1.41E-11	6.83E-12
75° to 80°	6.96E-11	4.22E-11	2.41E-11	1.37E-11	6.90E-12
80° to 85°	6.25E-11	3.70E-11	2.16E-11	1.22E-11	6.35E-12
85° to 90°	5.30E-11	3.26E-11	1.87E-11	1.10E-11	5.77E-12

Table 34 Cycles 6 and 7 Combined, dpa/s in Vessel Wall at Mid-height

Angle from Vertical	Distance Through Vessel Wall (T is wall thickness)				
	Inner Edge	T/4	T/2	3T/4	Outer Edge
0° to 5°	5.84E-11	3.47E-11	2.05E-11	1.16E-11	6.03E-12
5° to 10°	6.30E-11	3.71E-11	2.19E-11	1.25E-11	6.27E-12
10° to 15°	7.03E-11	4.14E-11	2.37E-11	1.32E-11	6.54E-12
15° to 20°	6.87E-11	4.03E-11	2.39E-11	1.28E-11	6.31E-12
20° to 25°	6.23E-11	3.72E-11	2.15E-11	1.23E-11	5.96E-12
25° to 30°	5.72E-11	3.44E-11	2.02E-11	1.17E-11	5.82E-12
30° to 35°	5.60E-11	3.34E-11	1.88E-11	1.06E-11	5.47E-12
35° to 40°	4.92E-11	2.84E-11	1.69E-11	9.37E-12	4.79E-12
40° to 45°	3.55E-11	2.15E-11	1.33E-11	7.68E-12	4.26E-12
45° to 50°	3.51E-11	2.22E-11	1.27E-11	7.57E-12	4.21E-12
50° to 55°	4.72E-11	2.86E-11	1.61E-11	9.27E-12	4.86E-12
55° to 60°	5.64E-11	3.36E-11	1.92E-11	1.09E-11	5.42E-12
60° to 65°	5.50E-11	3.20E-11	1.86E-11	1.12E-11	5.69E-12
65° to 70°	6.31E-11	3.66E-11	2.06E-11	1.19E-11	6.04E-12
70° to 75°	7.26E-11	4.26E-11	2.36E-11	1.36E-11	6.57E-12
75° to 80°	7.27E-11	4.33E-11	2.48E-11	1.37E-11	6.55E-12
80° to 85°	6.20E-11	3.74E-11	2.14E-11	1.21E-11	6.14E-12
85° to 90°	5.89E-11	3.40E-11	1.99E-11	1.15E-11	5.70E-12

Table 35 Cycle 8, dpa/s in Vessel Wall at Mid-height

Angle from Vertical	Distance Through Vessel Wall (T is wall thickness)				
	Inner Edge	T/4	T/2	3T/4	Outer Edge
0° to 5°	2.94E-11	1.84E-11	1.10E-11	6.59E-12	3.56E-12
5° to 10°	4.27E-11	2.48E-11	1.46E-11	8.44E-12	4.31E-12
10° to 15°	5.92E-11	3.40E-11	1.96E-11	1.10E-11	5.26E-12
15° to 20°	6.28E-11	3.70E-11	2.07E-11	1.16E-11	5.49E-12
20° to 25°	4.89E-11	2.91E-11	1.67E-11	9.49E-12	4.63E-12
25° to 30°	3.52E-11	2.06E-11	1.18E-11	7.05E-12	3.60E-12
30° to 35°	2.53E-11	1.53E-11	9.09E-12	5.45E-12	2.92E-12
35° to 40°	2.21E-11	1.31E-11	7.83E-12	4.70E-12	2.64E-12
40° to 45°	2.07E-11	1.22E-11	7.27E-12	4.29E-12	2.47E-12
45° to 50°	2.04E-11	1.20E-11	6.96E-12	4.22E-12	2.46E-12
50° to 55°	2.19E-11	1.28E-11	7.71E-12	4.58E-12	2.59E-12
55° to 60°	2.50E-11	1.51E-11	8.92E-12	5.30E-12	2.98E-12
60° to 65°	3.48E-11	2.04E-11	1.19E-11	6.92E-12	3.69E-12
65° to 70°	4.90E-11	2.89E-11	1.68E-11	9.55E-12	4.69E-12
70° to 75°	6.34E-11	3.67E-11	2.06E-11	1.15E-11	5.51E-12
75° to 80°	5.94E-11	3.44E-11	1.95E-11	1.09E-11	5.22E-12
80° to 85°	4.15E-11	2.49E-11	1.44E-11	8.33E-12	4.17E-12
85° to 90°	2.96E-11	1.81E-11	1.09E-11	6.43E-12	3.53E-12

Table 36 Cycle 9, dpa/s in Vessel Wall at Mid-height

Angle from Vertical	Distance Through Vessel Wall (T is wall thickness)				
	Inner Edge	T/4	T/2	3T/4	Outer Edge
0° to 5°	2.79E-11	1.72E-11	1.01E-11	5.85E-12	3.10E-12
5° to 10°	3.31E-11	1.91E-11	1.02E-11	6.63E-12	3.40E-12
10° to 15°	3.89E-11	2.29E-11	1.32E-11	7.62E-12	3.71E-12
15° to 20°	4.10E-11	2.36E-11	1.36E-11	7.71E-12	3.69E-12
20° to 25°	3.56E-11	2.05E-11	1.21E-11	6.92E-12	3.49E-12
25° to 30°	2.93E-11	1.75E-11	1.01E-11	5.83E-12	3.01E-12
30° to 35°	2.44E-11	1.43E-11	8.47E-12	4.94E-12	2.55E-12
35° to 40°	2.00E-11	1.20E-11	7.05E-12	4.18E-12	2.30E-12
40° to 45°	1.55E-11	9.61E-11	5.69E-12	3.56E-12	1.98E-12
45° to 50°	1.55E-11	9.34E-11	5.60E-12	3.38E-12	2.00E-12
50° to 55°	1.89E-11	1.13E-11	6.61E-12	3.94E-12	2.23E-12
55° to 60°	2.46E-11	1.44E-11	8.28E-12	4.83E-12	2.56E-12
60° to 65°	2.94E-11	1.73E-11	9.94E-12	5.69E-12	2.98E-12
65° to 70°	3.49E-11	2.02E-11	1.17E-11	6.80E-12	3.35E-12
70° to 75°	4.02E-11	2.35E-11	1.35E-11	7.59E-12	3.66E-12
75° to 80°	3.84E-11	2.25E-11	1.30E-11	7.34E-12	3.64E-12
80° to 85°	3.22E-11	1.92E-11	1.12E-11	6.55E-12	3.41E-12
85° to 90°	2.82E-11	1.67E-11	9.92E-12	5.74E-12	3.11E-12

Table 37 Cycle10, dpa/s in Vessel Wall at Mid-height

Angle from Vertical	Distance Through Vessel Wall (T is wall thickness)				
	Inner Edge	T/4	T/2	3T/4	Outer Edge
0° to 5°	2.11E-11	1.27E-11	7.56E-12	4.43E-12	2.48E-12
5° to 10°	2.43E-11	1.46E-11	8.67E-12	5.05E-12	2.57E-12
10° to 15°	2.92E-11	1.73E-11	1.02E-11	5.67E-12	2.78E-12
15° to 20°	3.04E-11	1.76E-11	1.03E-11	5.90E-12	2.89E-12
20° to 25°	2.77E-11	1.65E-11	9.55E-12	5.51E-12	2.76E-12
25° to 30°	2.65E-11	1.59E-11	9.08E-12	5.12E-12	2.63E-12
30° to 35°	2.42E-11	1.45E-11	8.48E-12	4.82E-12	2.43E-12
35° to 40°	2.01E-11	1.19E-11	7.11E-12	4.11E-12	2.15E-12
40° to 45°	1.66E-11	1.03E-11	6.14E-12	3.71E-12	2.00E-12
45° to 50°	1.78E-11	1.07E-11	6.23E-12	3.70E-12	1.99E-12
50° to 55°	2.06E-11	1.24E-11	7.30E-12	4.24E-12	2.23E-12
55° to 60°	2.39E-11	1.41E-11	8.15E-12	4.64E-12	2.38E-12
60° to 65°	2.52E-11	1.54E-11	8.70E-12	5.04E-12	2.59E-12
65° to 70°	2.68E-11	1.64E-11	9.58E-12	5.58E-12	2.80E-12
70° to 75°	2.99E-11	1.77E-11	1.04E-11	5.82E-12	2.92E-12
75° to 80°	2.92E-11	1.67E-11	9.86E-12	5.60E-12	2.85E-12
80° to 85°	2.45E-11	1.50E-11	8.74E-12	4.97E-12	2.52E-12
85° to 90°	2.02E-11	1.23E-11	7.37E-12	4.39E-12	2.33E-12

Table 38 Cycle 11, dpa/s in Vessel Wall at Mid-height

Angle from Vertical	Distance Through Vessel Wall (T is wall thickness)				
	Inner Edge	T/4	T/2	3T/4	Outer Edge
0° to 5°	1.91E-11	1.14E-11	6.53E-12	3.93E-12	2.03E-12
5° to 10°	2.21E-11	1.29E-11	7.51E-12	4.36E-12	2.18E-12
10° to 15°	2.46E-11	1.45E-11	8.39E-12	4.66E-12	2.41E-12
15° to 20°	2.42E-11	1.44E-11	8.35E-12	4.72E-12	2.39E-12
20° to 25°	2.19E-11	1.28E-11	7.64E-12	4.37E-12	2.26E-12
25° to 30°	2.01E-11	1.23E-11	7.21E-12	4.13E-12	2.22E-12
30° to 35°	1.94E-11	1.17E-11	6.83E-12	3.81E-12	1.99E-12
35° to 40°	1.61E-11	9.75E-12	5.65E-12	3.26E-12	1.78E-12
40° to 45°	1.34E-11	8.31E-12	4.85E-12	2.93E-12	1.67E-12
45° to 50°	1.39E-11	8.37E-12	4.90E-12	2.96E-12	1.64E-12
50° to 55°	1.71E-11	1.00E-11	5.79E-12	3.35E-12	1.79E-12
55° to 60°	1.96E-11	1.18E-11	6.85E-12	3.93E-12	2.05E-12
60° to 65°	2.13E-11	1.24E-11	7.41E-12	4.22E-12	2.19E-12
65° to 70°	2.26E-11	1.38E-11	8.17E-12	4.56E-12	2.33E-12
70° to 75°	2.76E-11	1.58E-11	9.03E-12	5.15E-12	2.57E-12
75° to 80°	2.74E-11	1.64E-11	9.17E-12	5.27E-12	2.58E-12
80° to 85°	2.30E-11	1.37E-11	8.02E-12	4.65E-12	2.39E-12
85° to 90°	1.89E-11	1.14E-11	6.79E-12	3.95E-12	2.13E-12

Table 39 Fluence to End of Cycle 11, Flux>0.1MeV in Vessel Wall at Mid-height

Angle from Vertical	Distance Through Vessel Wall (T is wall thickness)				
	Inner Edge	T/4	T/2	3T/4	Outer Edge
0° to 5°	2.20E+19	1.80E+19	1.32E+19	8.96E+18	5.12E+18
5° to 10°	2.48E+19	2.00E+19	1.46E+19	9.83E+18	5.52E+18
10° to 15°	2.90E+19	2.33E+19	1.67E+19	1.09E+19	6.01E+18
15° to 20°	3.02E+19	2.40E+19	1.71E+19	1.11E+19	6.06E+18
20° to 25°	2.62E+19	2.10E+19	1.51E+19	1.01E+19	5.60E+18
25° to 30°	2.27E+19	1.87E+19	1.36E+19	9.05E+18	5.11E+18
30° to 35°	2.21E+19	1.77E+19	1.27E+19	8.44E+18	4.86E+18
35° to 40°	1.90E+19	1.53E+19	1.12E+19	7.50E+18	4.36E+18
40° to 45°	1.47E+19	1.23E+19	9.17E+18	6.39E+18	3.87E+18
45° to 50°	1.45E+19	1.22E+19	9.12E+18	6.38E+18	3.98E+18
50° to 55°	1.91E+19	1.53E+19	1.10E+19	7.56E+18	4.45E+18
55° to 60°	2.26E+19	1.80E+19	1.29E+19	8.57E+18	4.92E+18
60° to 65°	2.30E+19	1.87E+19	1.34E+19	9.09E+18	5.21E+18
65° to 70°	2.58E+19	2.11E+19	1.51E+19	1.01E+19	5.65E+18
70° to 75°	3.04E+19	2.41E+19	1.70E+19	1.12E+19	6.06E+18
75° to 80°	2.97E+19	2.36E+19	1.68E+19	1.10E+19	6.02E+18
80° to 85°	2.46E+19	2.01E+19	1.45E+19	9.74E+18	5.51E+18
85° to 90°	2.23E+19	1.81E+19	1.31E+19	8.80E+18	5.05E+18

Table 40 Fluence to End of Cycle 11, Flux>1.0MeV in Vessel Wall at Mid-height

Angle from Vertical	Distance Through Vessel Wall (T is wall thickness)				
	Inner Edge	T/4	T/2	3T/4	Outer Edge
0° to 5°	1.01E+19	5.60E+18	2.84E+18	1.31E+18	5.46E+17
5° to 10°	1.15E+19	6.23E+18	3.10E+18	1.46E+18	6.08E+17
10° to 15°	1.37E+19	7.35E+18	3.63E+18	1.66E+18	6.86E+17
15° to 20°	1.39E+19	7.47E+18	3.58E+18	1.67E+18	6.75E+17
20° to 25°	1.20E+19	6.42E+18	3.15E+18	1.47E+18	5.94E+17
25° to 30°	1.02E+19	5.61E+18	2.77E+18	1.31E+18	5.51E+17
30° to 35°	1.00E+19	5.47E+18	2.66E+18	1.24E+18	5.20E+17
35° to 40°	8.66E+18	4.74E+18	2.30E+18	1.06E+18	4.53E+17
40° to 45°	6.65E+18	3.71E+18	1.85E+18	8.83E+17	3.91E+17
45° to 50°	6.63E+18	3.66E+18	1.82E+18	8.69E+17	3.86E+17
50° to 55°	8.68E+18	4.75E+18	2.29E+18	1.09E+18	4.57E+17
55° to 60°	1.03E+19	5.64E+18	2.75E+18	1.28E+18	5.26E+17
60° to 65°	1.08E+19	5.75E+18	2.80E+18	1.31E+18	5.53E+17
65° to 70°	1.18E+19	6.44E+18	3.15E+18	1.49E+18	6.10E+17
70° to 75°	1.40E+19	7.58E+18	3.64E+18	1.70E+18	6.81E+17
75° to 80°	1.37E+19	7.40E+18	3.61E+18	1.69E+18	6.77E+17
80° to 85°	1.13E+19	6.24E+18	3.04E+18	1.42E+18	6.02E+17
85° to 90°	1.02E+19	5.50E+18	2.68E+18	1.29E+18	5.36E+17

Table 41 Exposures to End of Cycle 11, dpa in Vessel Wall at Mid-height

Angle from Vertical	Distance Through Vessel Wall (T is wall thickness)				
	Inner Edge	T/4	T/2	3T/4	Outer Edge
0° to 5°	1.49E-2	9.01E-3	5.34E-3	3.08E-3	1.59E-3
5° to 10°	1.70E-2	1.00E-2	5.95E-3	3.42E-3	1.74E-3
10° to 15°	1.99E-2	1.18E-2	6.80E-3	3.81E-3	1.90E-3
15° to 20°	2.03E-2	1.19E-2	6.87E-3	3.87E-3	1.91E-3
20° to 25°	1.75E-2	1.04E-2	6.07E-3	3.48E-3	1.75E-3
25° to 30°	1.52E-2	9.21E-3	5.40E-3	3.10E-3	1.59E-3
30° to 35°	1.48E-2	8.80E-3	5.10E-3	2.91E-3	1.51E-3
35° to 40°	1.28E-2	7.62E-3	4.45E-3	2.56E-3	1.34E-3
40° to 45°	9.91E-3	6.06E-3	3.63E-3	2.16E-3	1.19E-3
45° to 50°	9.89E-3	6.03E-3	3.60E-3	2.15E-3	1.21E-3
50° to 55°	1.28E-2	7.62E-3	4.39E-3	2.58E-3	1.38E-3
55° to 60°	1.52E-2	9.01E-3	5.21E-3	2.97E-3	1.54E-3
60° to 65°	1.57E-2	9.25E-3	5.38E-3	3.12E-3	1.63E-3
65° to 70°	1.75E-2	1.05E-2	6.09E-3	3.50E-3	1.77E-3
70° to 75°	2.07E-2	1.21E-2	6.89E-3	3.92E-3	1.91E-3
75° to 80°	2.01E-2	1.19E-2	6.84E-3	3.84E-3	1.90E-3
80° to 85°	1.68E-2	1.02E-2	5.88E-3	3.38E-3	1.74E-3
85° to 90°	1.51E-2	9.02E-3	5.28E-3	3.05E-3	1.58E-3

Figure 1 Scan Down the Palisades Reactor

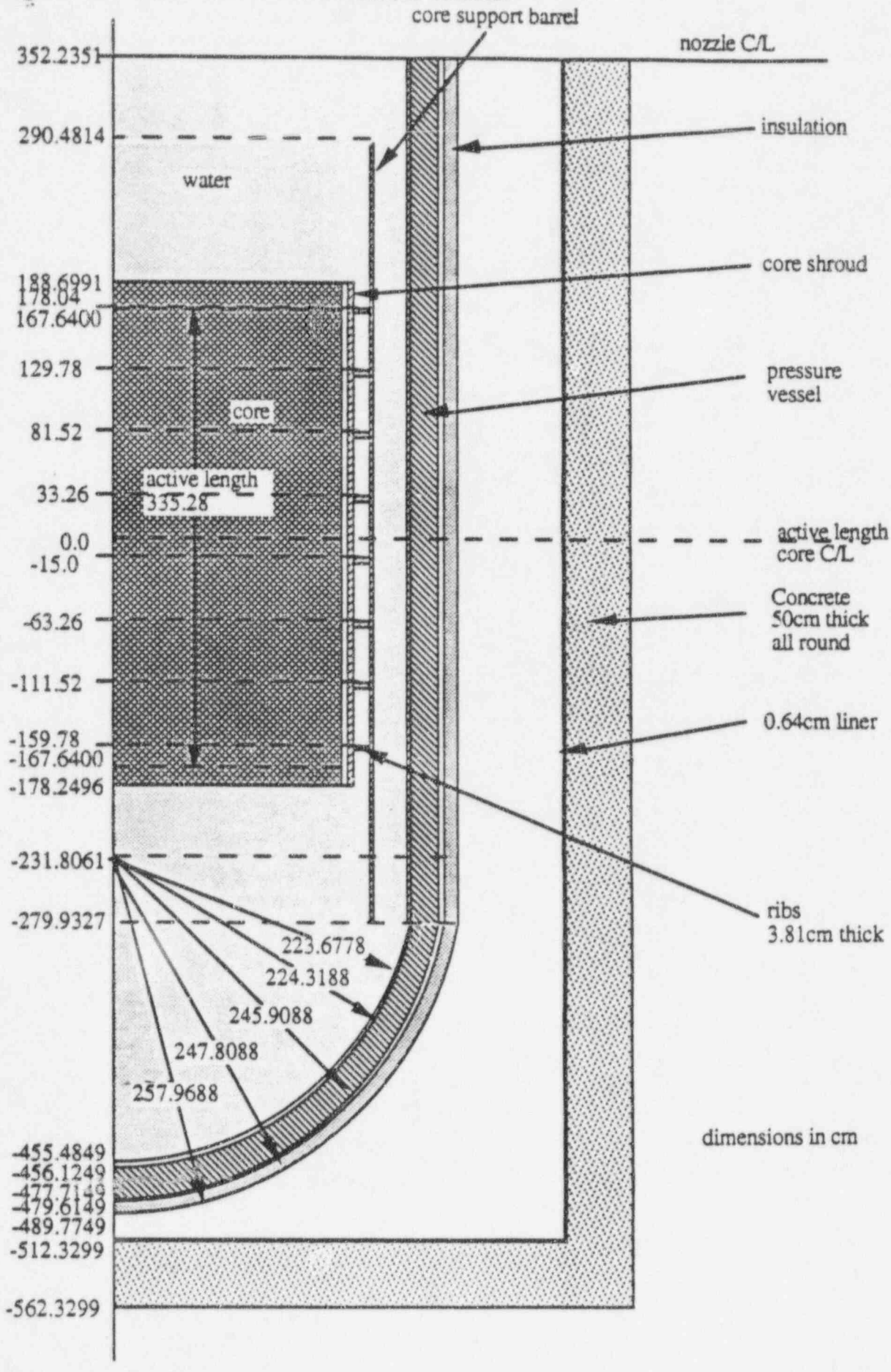

Figure 2 Plan View Across a Quarter Section of the Palisades Reactor

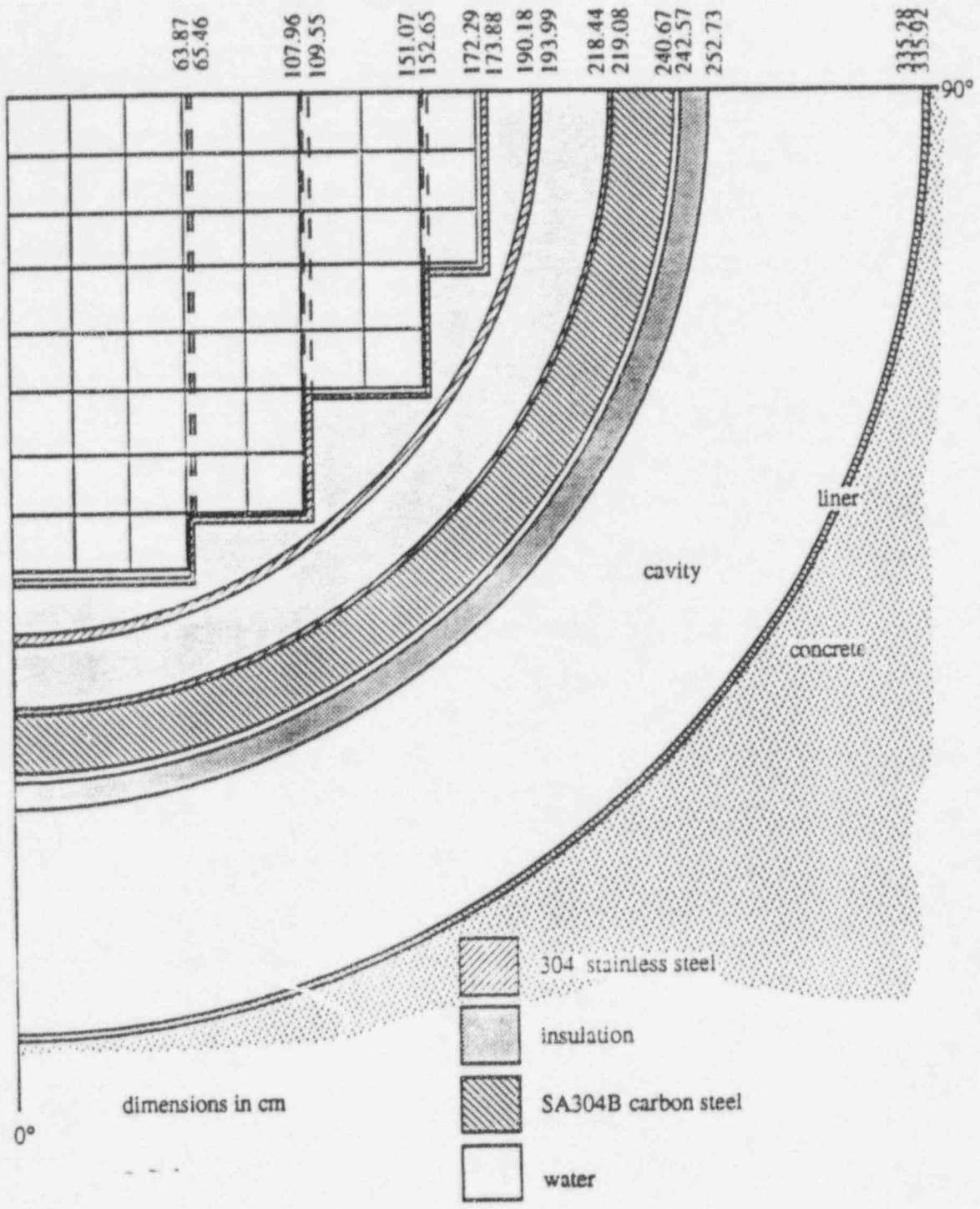

Figure 3 Arrangement of Fuel Elements in the Reactor Core

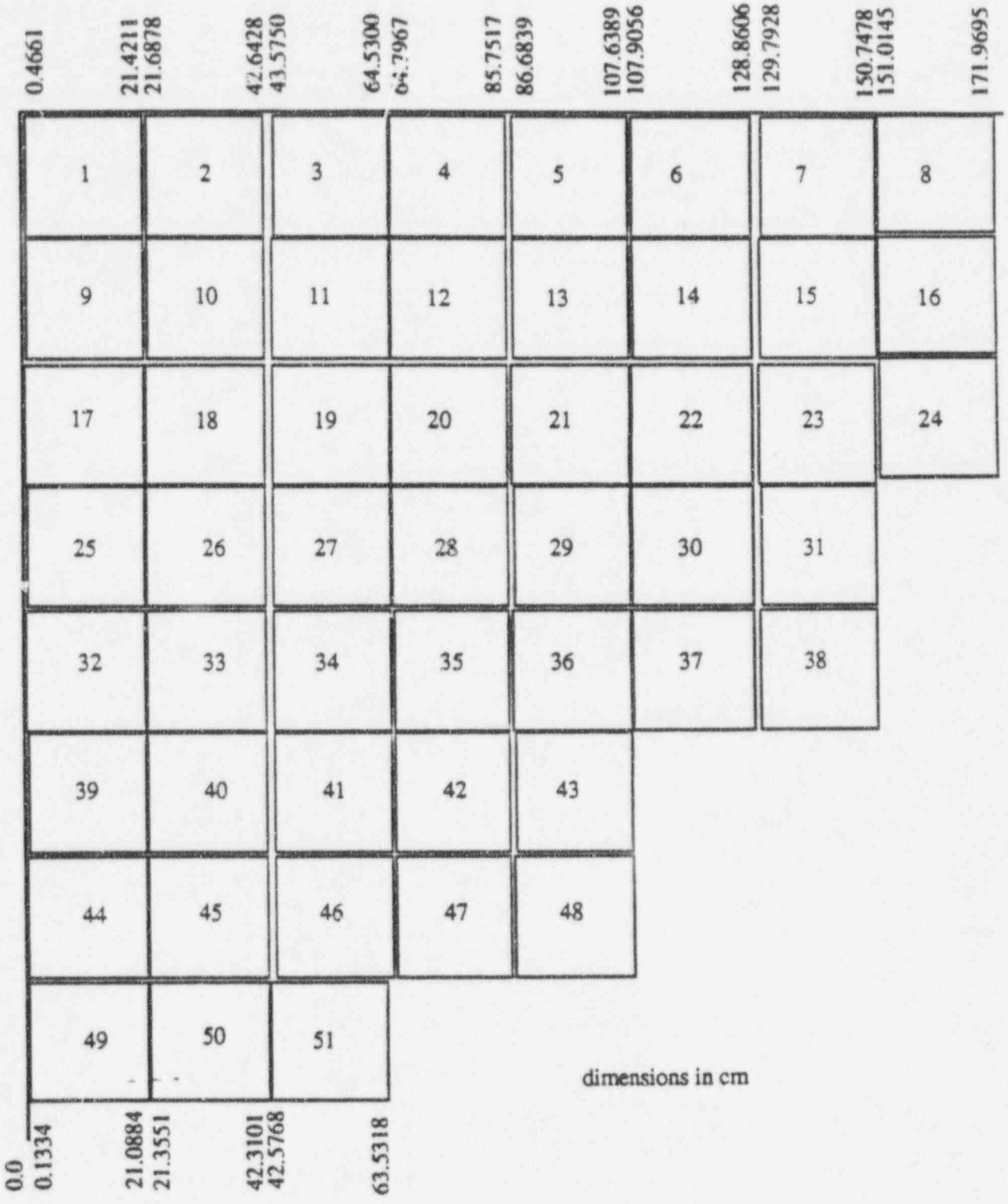

Figure 4 Section Across a Fuel Element with 216 Fuel Pins

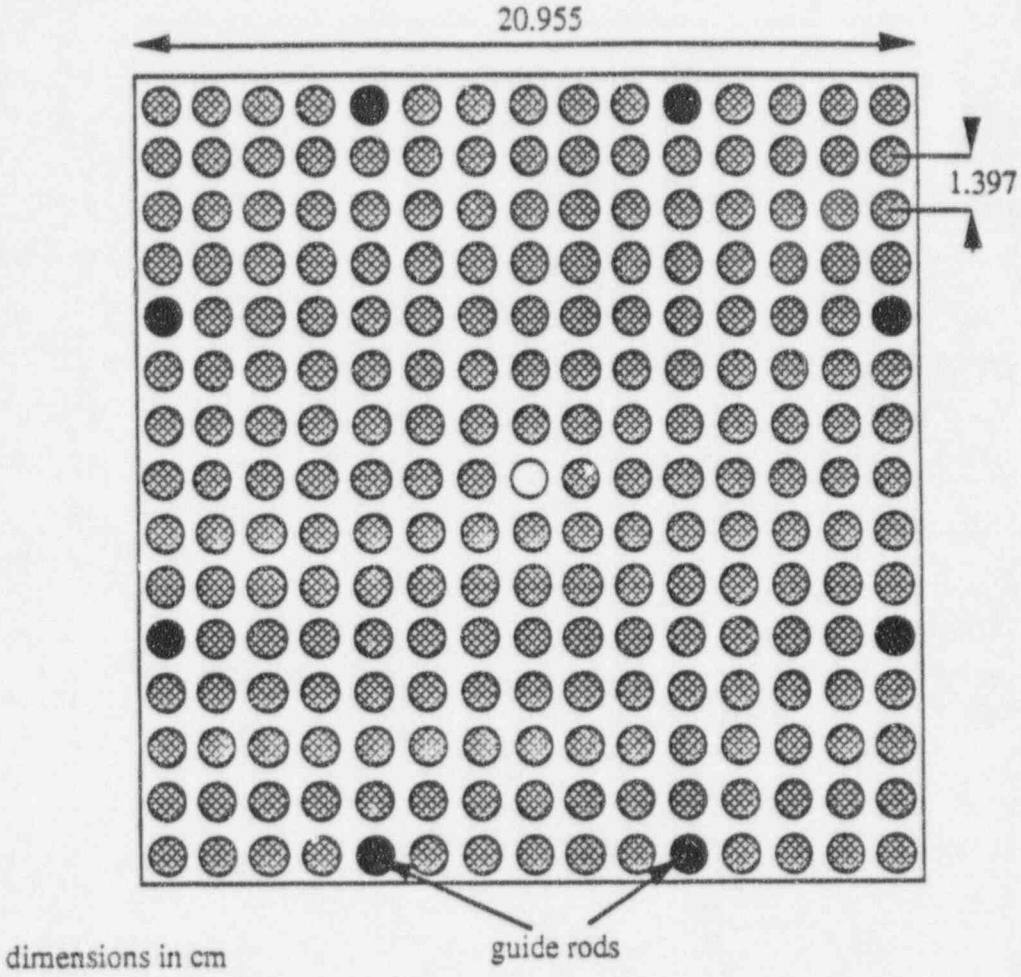

Fuel Element

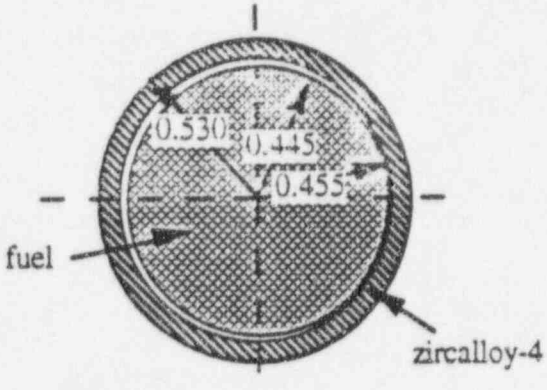

Fuel Pin

Figure 5 Fuel Element Arrangement

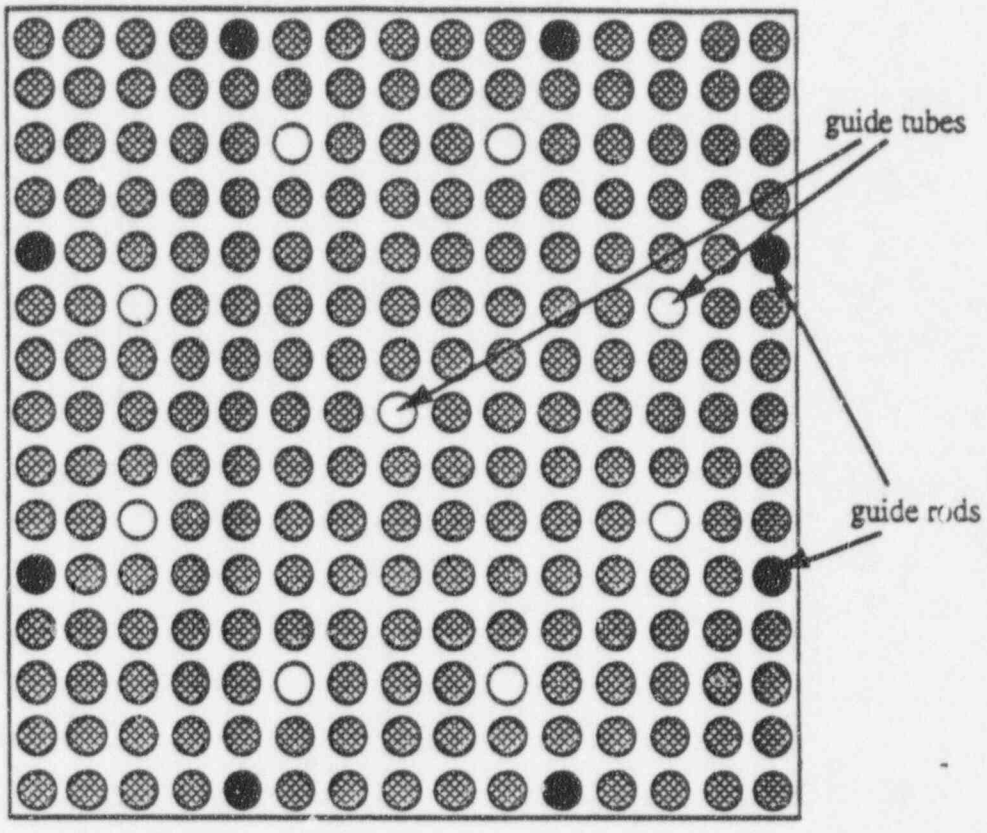

5(a) 208 fuel pins in assembly

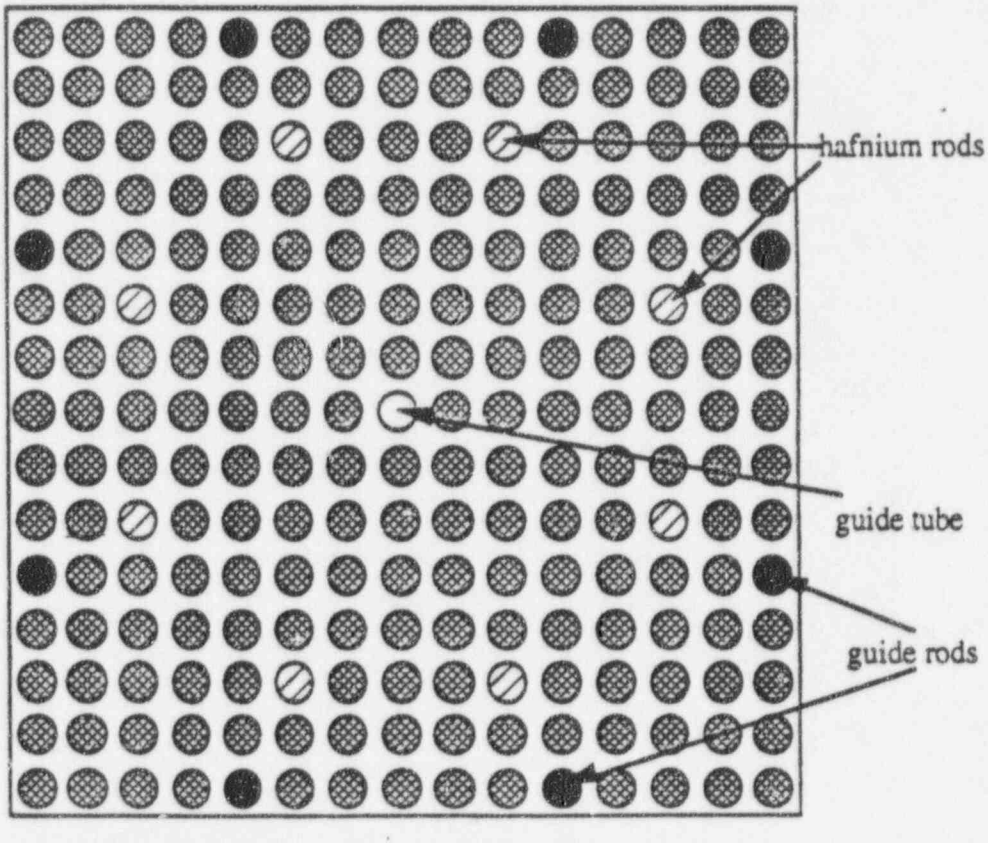

5(b) 208 fuel pins with 8 hafnium rods

Figure 5 Fuel Element Arrangement (continued)

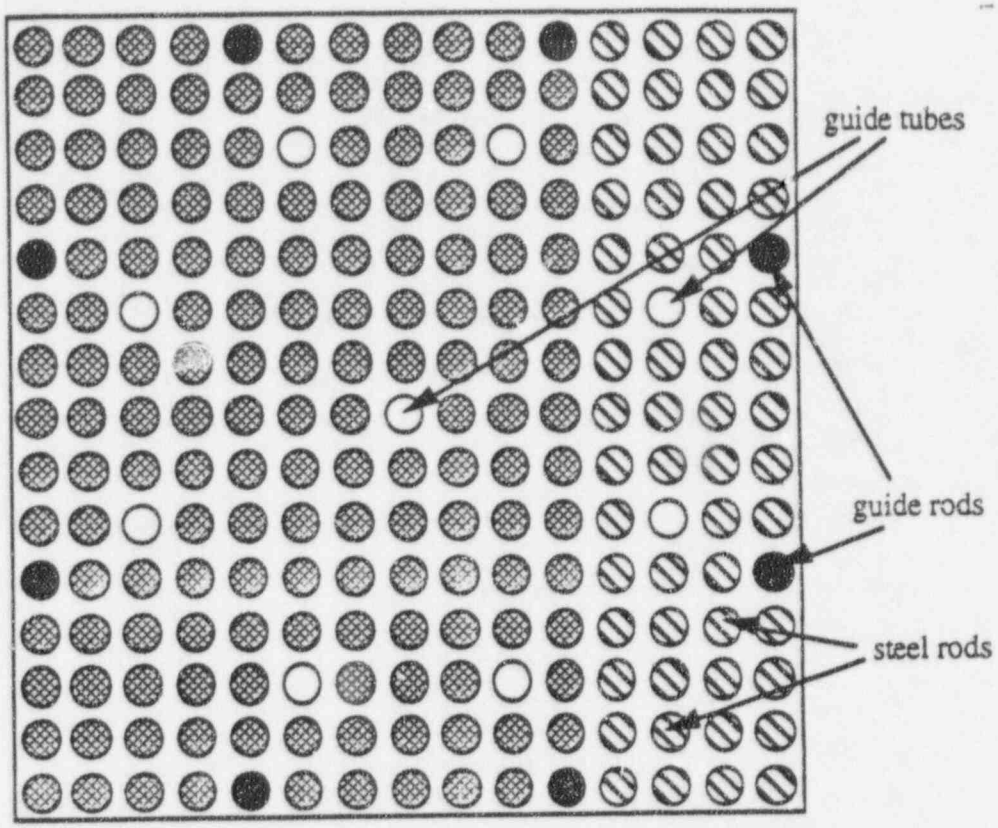

5(c) 152 fuel pins with steel rods on one side

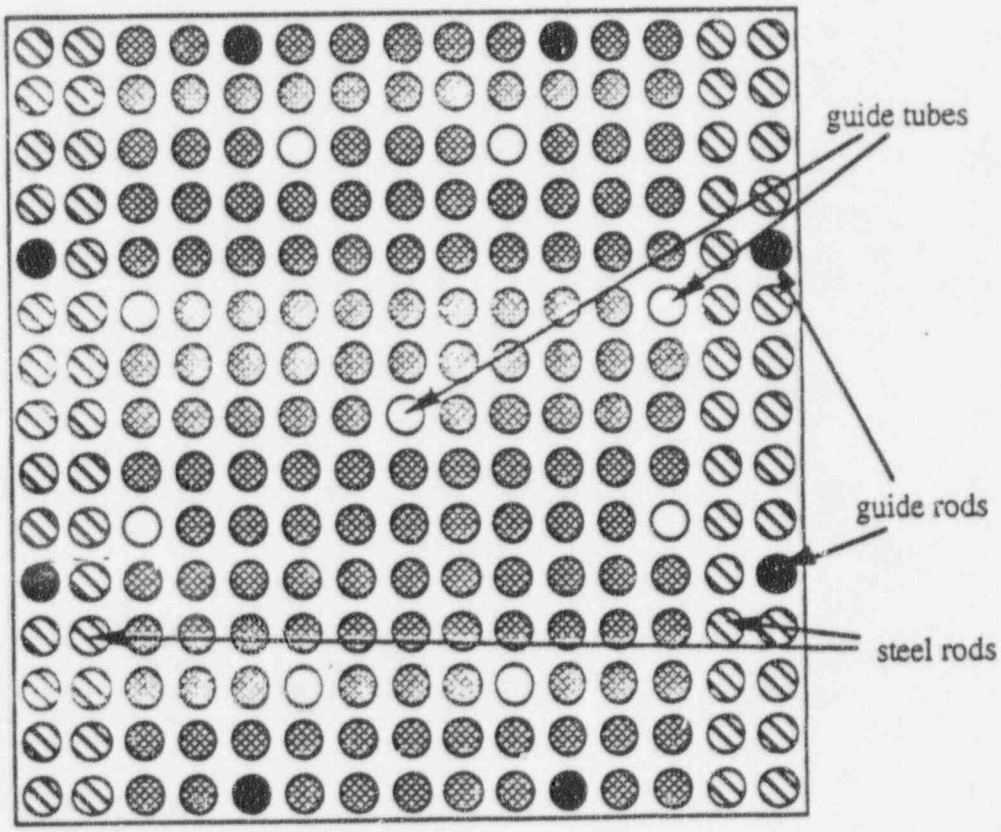

5(d) 160 fuel pins with steel rods on both sides

Figure 5 Fuel Element Arrangement (continued)

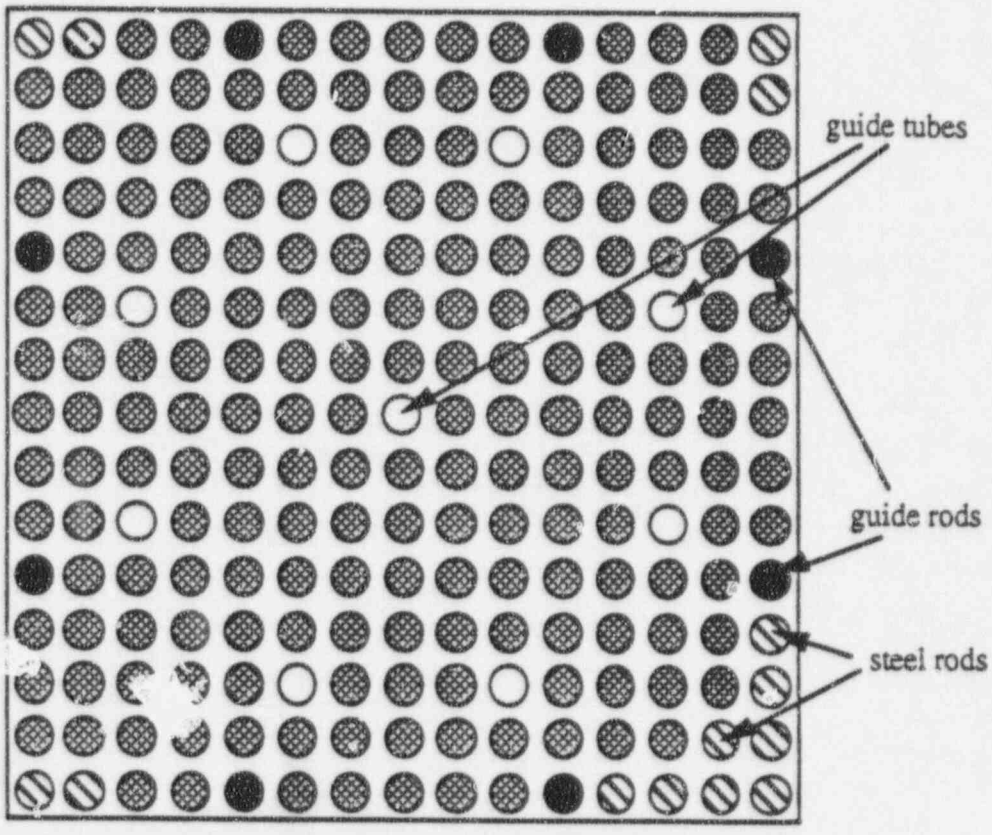

5(e) 194 fuel pins with steel rods in corners

Figure 6 Drawing of Surveillance and Accelerated Capsules

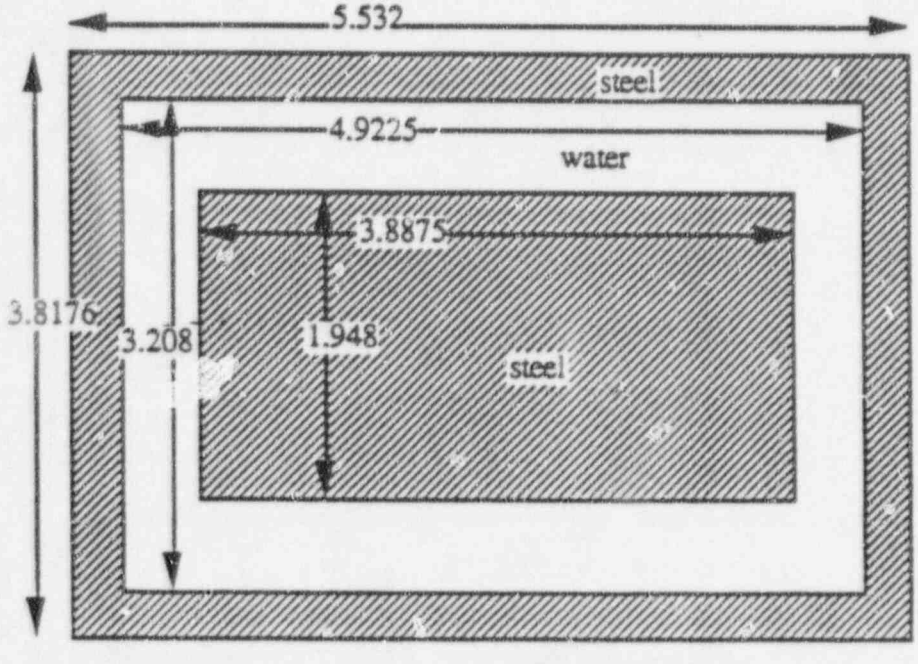

Dimensions in cm

Distribution

R Snuggerud (10 Copies)	Consumers Power, Palisades Plant, 27780 Blue Star Memorial Highway, Covert, MI 49043, USA.
D Spaar	AEAT E.S. Inc., 241 Curry Hollow Road,Pittsburgh, PA15236, USA
A F Avery	30''/A32 Winfrith
Miss W V Wright	309/A32 Winfrith
Dr I J Curl	357/A32 Winfrith
AEAT Archive (2 copies)	Bdg 149, Harwell
RPSCD Database (Mrs L J Neal)	316/A32 Winfrith